Wilkens, R.H., Firth, J., Bender, J., et al., 1993
Proceedings of the Ocean Drilling Program, Scientific Results, Vol. 136

10. THE AGE AND ALTERATION OF CENTRAL PACIFIC OCEANIC CRUST NEAR HAWAII, SITE 843[1]

David Guy Waggoner[2]

ABSTRACT

^{40}Ar–^{39}Ar incremental heating experiments on a relatively unaltered basalt from Site 843 yield a crystallization age of 110 ± 2 Ma for the central Pacific Ocean igneous basement near Hawaii. Previous estimates of the age of the basement inferred by indirect methods and from radiometric dates of the South Hawaiian Seamounts are too young by 20–30 m.y. Phyllosilicate alteration minerals from veins in the Site 843 basalts define a Rb/Sr isochron with an age of 94.5 ± 0.5 Ma. The isochron records the last equilibration of the phyllosilicate minerals with a hydrothermal fluid at about 16 m.y. after the formation of the igneous basement. The last event recorded by calcite veins is the sealing of the crust by a sufficient thickness of sediment to impede the free circulation of seawater into the crust. The chemistry of the alteration minerals indicates the rare earth elements in the hydrothermal solutions were derived from alteration of the basalts and, furthermore, were transported in solution as metal species and carbonate complexes. Calcite with approximately seawater $^{87}Sr/^{86}Sr$, but Sr contents too low to precipitate directly from seawater, is suggested to have formed at a late stage in the alteration history of the crust by the reaction of seawater with calcite precipitated earlier from basalt-dominated hydrothermal fluids.

INTRODUCTION

The basalts recovered at Ocean Drilling Program (ODP) Site 843 in the central Pacific Ocean are the first samples of igneous basement from near the Hawaiian Islands (Fig. 1). The site is located on the Hawaiian Arch (a recent tectonic feature) about 320 km west of the big island of Hawaii and about 225 km south–southwest of the island of Oahu (Fig. 1). The middle Cretaceous basement rocks recovered at Site 843 are probably representative of the oceanic crust through which lavas of the Hawaiian mantle plume have ascended to form the islands from Oahu to Hawaii. These islands are recent in origin, having formed in the last 4 m.y. as the Pacific Plate drifted northwestward over a stationary melting anomaly in the mantle (e.g., Clague and Dalrymple, 1987). Among the goals of Leg 136 were the determination of the age and general characteristics of the oceanic crust in the central Pacific Ocean near the Hawaiian Islands.

Many of the physical and geochemical properties of the oceanic crust are directly related to its age. To characterize oceanic crust for geophysical and geodynamic modeling, it is necessary to study crust produced at both fast- and slow-spreading ridges and at different stages of maturity. The ocean crust at Site 843 was produced at fast-spreading rates of about 100 mm/yr along the Pacific/Farallon plate boundary sometime during the middle Cretaceous (e.g., Engebretson et al., 1985). The crust at Site 843 thus provides a complement and contrast to the crust at Site 417/418 produced at the slow-spreading Mid-Atlantic Ridge during the same time period. Previous studies of the crust at Site 417/418 have influenced many of our ideas about how the oceanic crust ages (e.g., Donnelly, Francheteau, et al., 1979; Hart and Staudigel, 1979; Alt and Honnorez, 1984; Staudigel and Hart, 1985).

Before the sampling conducted during Leg 136, the age of the oceanic crust around the Hawaiian Islands was poorly known because the crust formed during the Cretaceous normal polarity superchron (119 to 83 Ma). Previous age estimates have ranged from 80 to 110 Ma (e.g., Epp, 1978, 1984; Sager and Pringle, 1987). These age estimates were based on indirect methods either by extrapolations from identified marine magnetic anomalies at considerable distance from Hawaii or by radiometric age determinations on dredged seamount samples assumed to have erupted shortly after oceanic crust formation. Shipboard paleontologic analysis of nannofossils in sediments directly overlying the basalts provides a minimum age for the basement of 94 to 100 Ma (Dziewonski, Wilkens, Firth, et al., 1992).

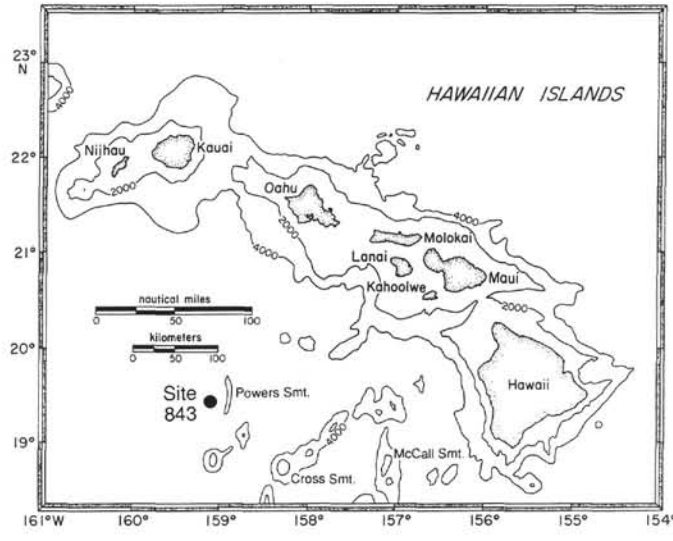

Figure 1. Map of the Hawaiian Islands showing the location of Site 843 in the central Pacific Ocean. Bathymetric contours are in meters.

Among the indirect age estimates for the crust beneath the Hawaiian Islands extrapolated from marine magnetic anomalies, the 92 to 94 Ma estimate of Epp (1978, 1984) is often quoted in the literature. This estimate is based on the position of the edge of the magnetic quiet zone to the east and identified younger marine magnetic anomalies to the southeast. Error estimates for extrapolations are often substantial (10 m.y. or more) because of the many assumptions that are required concerning spreading rates and the identification and age of magnetic anomalies. Substantial errors are also inherent in plate reconstruction models that form the basis of indirect age estimates.

Sager and Pringle (1987) analyzed the ages of a number of Cretaceous seamounts in the immediate vicinity of the Hawaiian Islands, principally by ^{40}Ar–^{39}Ar methods. These authors obtained ages that range from 70 to 90 Ma, with the most reliable ages near Site 843 between 80 Ma and 90 Ma. For seamount age estimates to

[1] Wilkens, R.H., Firth, J., Bender, J., et al., 1993. *Proc. ODP, Sci. Results,* 136: College Station, TX (Ocean Drilling Program).

[2] Hawaii Institute of Geophysics, University of Hawaii, Honolulu, HI 96822, U.S.A.

place meaningful limits on the age of the underlying crust, however, the seamounts must be erupted near the ridge crest. Studies of lithospheric flexure and compensation for Cretaceous seamounts near the Hawaiian Islands suggest that these volcanic edifices were constructed in a variety of settings ranging from near ridge to well off axis (e.g., Watts et al., 1980; Schwank and Lazarewicz, 1982; Freedman and Parson, 1986).

Thermally driven convection of seawater through the oceanic crust at actively spreading ridge crests is a well-established fact (e.g., Wolery and Sleep, 1976; Anderson et al., 1977; Corliss et al., 1979; Edmond et al., 1979). Radiometric dating of alteration minerals produced during the alteration of the oceanic crust has shown that the duration of the chemically active phase of hydrothermal circulation is short-lived, usually lasting no longer than 10 to 20 m.y. after crust formation (e.g., Hart and Staudigel, 1978, 1979; Richardson et al., 1980; Staudigel et al., 1981; Duncan et al., 1984: Staudigel and Hart, 1985; Peterson et al., 1986; Staudigel et al., 1986; Staudigel and Gillis, 1990). There are exceptions to the 10 to 20 m.y. limit. ^{40}Ar–^{39}Ar studies of vein minerals in the Troodos ophiolite have shown that hydrothermal circulation can last up to 30 m.y. after crust formation (Gallahan and Duncan, 1991). In settings where off-axis volcanism occurred, vein minerals can record ages for alteration events that are considerably younger (up to 50 m.y.) than the age of crust formation (Hart and Staudigel, 1986; LeHuray and Johnson, 1989).

The extent to which the alteration of igneous minerals and cementation of voids and cracks by alteration products continues beyond the stage of active hydrothermal circulation is still uncertain. Studies of oxygen isotopes in pore waters from sediments directly overlying basalts suggest that exchange between the oceanic crust and seawater may continue beyond 20 m.y. to as much as 120 m.y. (e.g., Lawrence et al., 1975; Lawrence and Gieskes, 1981). Studies of the seismic structure of the oceanic crust also suggest continued alteration processes beyond 20 m.y. after crust formation. The basaltic Layer 2 of young oceanic crust can be subdivided into an upper, low-velocity Layer 2A and a deeper, high-velocity Layer 2B (e.g., Christensen and Salisbury, 1972; Houtz and Ewing, 1976). The depth of the boundary between Layers 2A and 2B becomes shallower with increasing age of the oceanic crust, and generally Layer 2A disappears completely between crustal ages of 40 and 70 m.y. (Ewing and Houtz, 1979). The disappearance of Layer 2A is attributed to filling of cracks and voids with secondary minerals during hydrothermal circulation and diagenesis in the crust (e.g., Houtz and Ewing, 1976; Anderson et al., 1977; Wilkens et al., 1991; Jacobson, 1992).

The remainder of this paper is divided into two parts. First, a ^{40}Ar–^{39}Ar radiometric age for the formation of the basaltic ocean crust at Site 843 is presented, along with a summary discussion of the implications of this new date. The second part presents the Rb–Sr systematics and geochemical analyses of alteration minerals in the basalts, and discusses the implications of these results for alteration processes in the oceanic crust at Site 843.

^{40}Ar–^{39}Ar GEOCHRONOLOGY OF BASALTS

Samples and Analytical Methods

Shipboard descriptions of cores and thin sections of Site 843 basalts are given by Dziewonski, Wilkens, Firth, et al. (1992). A detailed petrochemical study of the Site 843 basalts is presented by King et al. (this volume). All the Site 843 basalts are quartz normative tholeiites based on X-ray fluorescence (XRF) analysis of major elements and similar to most other mid-ocean-ridge basalts (MORB). Isotope and trace element analyses also suggest an affinity with MORB (King et al., this volume).

However, some trace element ratios (i.e., very low La/Nb, very low Ba/Nb, and large positive Eu anomalies) suggest some unusual mantle source characteristics for these basalts compared with those of normal MORB (see King et al., this volume).

The basalt used for ^{40}Ar–^{39}Ar dating is from Sample 136-843B-1R-1, 15–17 cm, near the top of the cored section and about 18 m into basement (Fig. 2). It has relatively high K_2O (0.16 wt%) and high Rb (1.1 ppm) compared with normal MORB, possibly the result of alteration (e.g., Alt, this volume). The initial $^{87}Sr/^{86}Sr$ ratio of 0.70268 calculated for this basalt at 110 Ma is only slightly higher than the initial $^{87}Sr/^{86}Sr$ ratio of 0.70260 at 110 Ma estimated for this suite of basalts (see "Implications of Vein Minerals for Hydrothermal Processes" section, this chapter). The low initial $^{87}Sr/^{86}Sr$ ratio indicates this basalt is only slightly altered, and both the high K_2O and high Rb contents are characteristics of the magma. Petrographic examination reveals only slight alteration of the major igneous minerals in the basalt, with no alteration of groundmass plagioclase or clinopyroxene

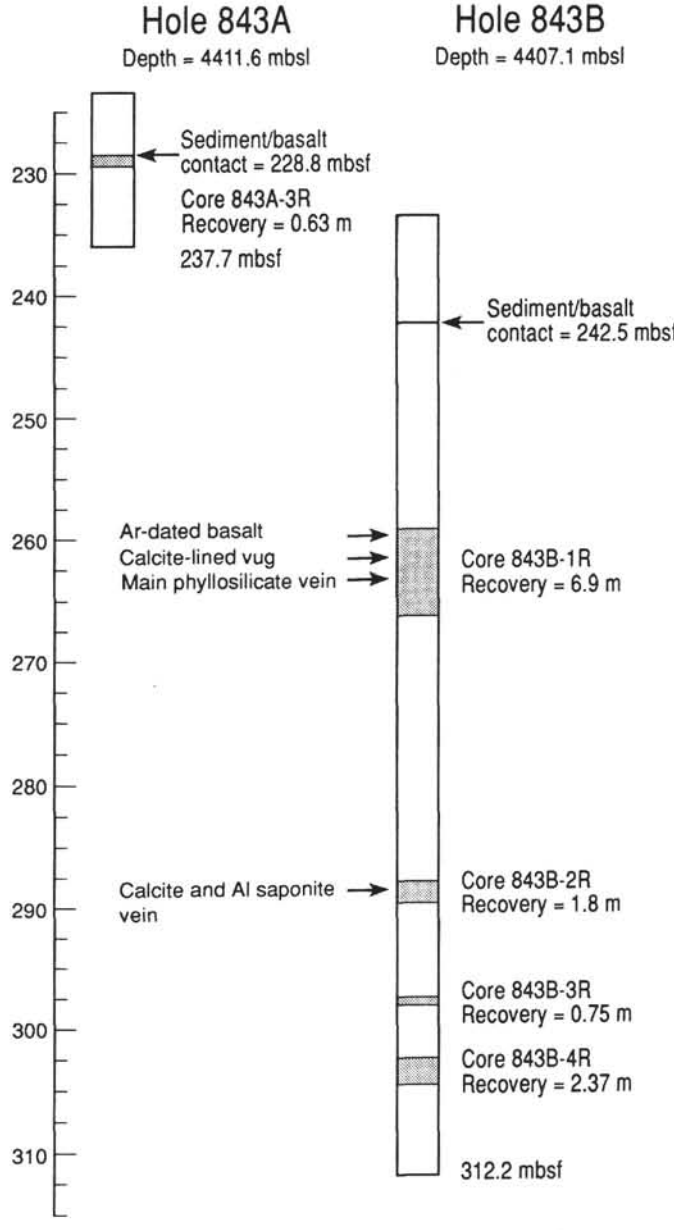

Figure 2. Diagram of the cored intervals in basement at Site 843 indicating where basalts were recovered in Holes 843A and 843B, after Dziewonski, Wilkens, Firth, et al. (1992). Arrows indicate locations of samples used in this study. Shaded areas indicate intervals of basalt recovery. mbsl = meters below sea level. mbsf = meters below seafloor.

and only 40% alteration of olivine. On the other hand, the less abundant interstitial glass (9% by volume) is about 90% altered. The combined petrographic, chemical, and isotopic characteristics suggest that only minor alteration of the sample has occurred.

The basalt is from the interior of a flow where vesicularity is about 1%; moreover, most of the basalts examined at this site have low vesicularity. The basalt comes from a long core interval of megascopically uniform basalt without chilled margins, which suggests a massive flow. Large blocky plagioclase phenocrysts in the basalt show an undulatory extinction, also suggesting deformation of a massive flow. In addition, a late-stage segregation of finer-grained plagioclase, olivine, and clinopyroxene crystals is observed. The massive nature of the flow, low vesicularity, and estimated 1700 to 2000 m eruption depth (based on the model of Sclater, et al., 1971) may have resulted in incomplete outgassing of the lava. Incomplete outgassing of magmatic Ar isotopes can result in an inherited $^{40}Ar/^{36}Ar$ component in the basalt rather than the atmospheric ratios normally assumed.

To establish the age of the igneous basement at Site 843, ^{40}Ar–^{39}Ar incremental heating techniques were employed. The ^{40}Ar–^{39}Ar method is a variation of the K–Ar method that relies on neutron irradiation of samples to produce ^{39}Ar from ^{39}K. Subsequent incremental heating of the irradiated sample in a vacuum to the point of total fusion allows extraction of parent (^{39}Ar, proportional to K content) and daughter (^{40}Ar) isotopes during each discrete temperature step. For a summary of the method, see McDougall and Harrison (1988) and Faure (1986).

The basalt from Sample 136-843B-1R-1, 15–17 cm, was prepared for analysis by grinding off saw and drill marks using Al grit, followed by repeated cleaning in deionized water in an ultrasonic bath. The dried sample was then crushed between motor-driven tungsten carbide plates and a 0.5- to 1-mm-sized fraction was separated. This fraction was hand-picked to remove vein- and vesicle-filling alteration products and then ultrasonically washed in distilled water. An approximately 0.5-g split of the prepared whole-rock chips was sealed in an evacuated quartz tube and irradiated for 8 hr in the core of the Oregon State University TRIGA reactor, where it received a neutron dose of $\sim 0.7 \times 10^{18}$ nvt. The efficiency of conversion of ^{39}K to ^{39}Ar by neutron capture was monitored with samples of hornblende standard Mmhb-1 (520.4 ± 1.7 Ma; Samson and Alexander, 1987). Further details of the flux characteristics, monitor minerals, and corrections for interfering K- and Ca-derived Ar isotopes are given by Dalrymple et al. (1981).

The Ar isotopic analyses were carried out in the laboratory of R. Duncan at Oregon State University. Ar extractions were performed in a conventional high-vacuum glass line using radio frequency induction heating. Heating steps were set from power levels on the generator determined from previous experience to divide the total whole-rock Ar into six roughly equal portions. Samples were held at each temperature-step setting for 30 min. The Ar isotopic composition of each increment was measured with an AEI MS-10S mass spectrometer with computer-controlled peak switching and data acquisition. The system blank was 3×10^{-14} moles ^{40}Ar. Decay constants used are those of Steiger and Jäger (1977).

Results

Results of the ^{40}Ar–^{39}Ar incremental heating experiment on the basalt from Sample 136-843B-1R-1, 15–17 cm, are shown in Figure 3A as an age-spectra diagram, in which the ages calculated from the composition of the gas in each heating step are plotted against the cumulative gas released (% ^{39}Ar). All six of the heating steps have concordant ages within the analytical errors. However, because the lowest temperature increment has extremely large analytical uncertainty and represents less than 5% of the total gas released, it was not included in calculation of the plateau age. The weighted mean of the five higher-temperature steps gives a plateau age of 107 ± 5 Ma for greater than 95% of the total gas released.

The Ar isotopic compositions for the various heating steps can also be correlated in an isochron diagram (Fig. 3B) in which isotopic ratios

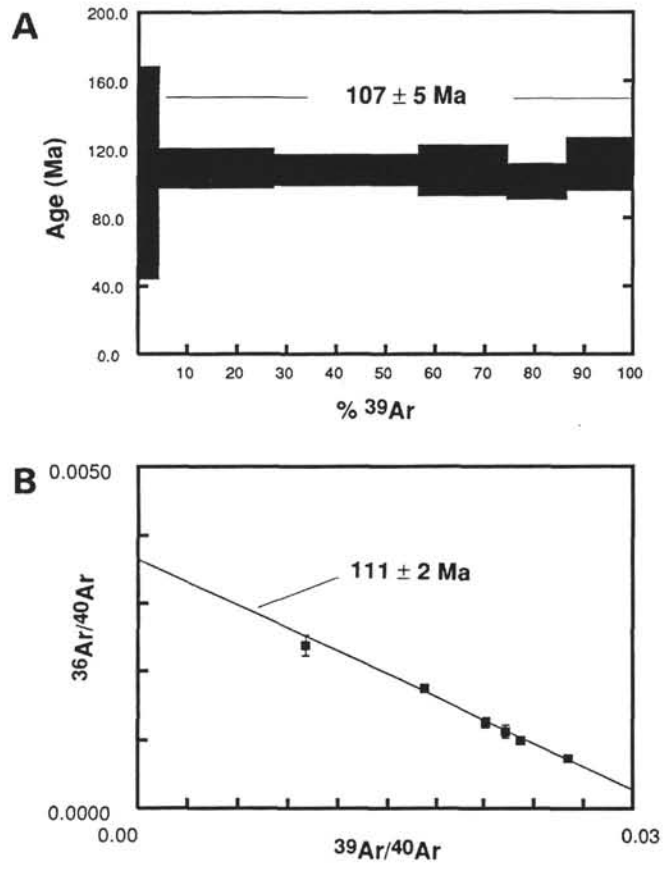

Figure 3. **A.** Apparent age spectra diagram for ^{40}Ar–^{39}Ar incremental heating experiments on a relatively unaltered basalt, Sample 136-843B-1R-1,15–17 cm. Horizontal boxes indicate the age estimate with analytical error (±1σ) for each heating step as a percentage of the total gas released (% ^{39}Ar). A weighted mean of the five higher-temperature steps yields the plateau age for the basalt indicated. **B.** Isochron diagram for the ^{40}Ar–^{39}Ar incremental heating experiments on the same basalt plotting $^{36}Ar/^{40}Ar$ vs. $^{39}Ar/^{40}Ar$ for the six gas release steps. The isochron age was calculated from the slope of the line fitted by least-squares methods using the analytical uncertainties (York, 1969). The $^{36}Ar/^{40}Ar$ intercept is 0.003645 ± 0.000151, which corresponds to a $^{40}Ar/^{36}Ar$ of 274.3 ± 11.4, somewhat lower than the atmospheric value of 295.5.

vs. their parent to daughter ratios are plotted. When a set of collinear points in an isochron diagram is fitted by least-squares methods, it yields a slope, which determines an isochron's age, and an intercept, which defines the isotopic composition of Ar in the sample when it crystallized. In contrast to the age-spectra plots, which usually assume an initial $^{40}Ar/^{36}Ar$ composition equal to the atmospheric value of 295.5, the isochron diagram allows independent determination of sample age and initial $^{40}Ar/^{36}Ar$. The isochron correlation for this basalt yields an age of 111 ± 2 Ma with an $^{40}Ar/^{36}Ar$ intercept of 274.3 ± 11.4 (Fig. 3B).

The criteria of Lanphere and Dalrymple (1978), Dalrymple et al. (1980), and Pringle (1992) are used to evaluate whether this basalt is too disturbed or altered to yield a reliable, independent crystallization age. These criteria are (1) a well-defined high-temperature age-spectrum-plateau formed by three or more concordant, contiguous steps representing at least 50% of the ^{39}Ar released (already discussed); (2) a well-defined isochron for the plateau points with a F-variate statistic [SUMS/(N – 2)] sufficiently low at the 95% confidence level; (3) plateau and isochron ages concordant at the 95% confidence level; and (4) an $^{40}Ar/^{36}Ar$ intercept on the isochron diagram not significantly different from the atmospheric value of 295.5 at the 95% confidence level.

The goodness-of-fit parameter SUMS (York, 1969) is 2.22 for the isochron regression (Fig. 3B). The F-variate statistic SUMS/($N-2$) (i.e., the ratio of total scatter about the isochron to the scatter attributable to analytical errors alone) is 0.56 for these six data points. A F-variate statistic less than 2.37, for a regression fitted with six steps, indicates an isochron relationship cannot be rejected at the 95% confidence level. To meet the criteria of concordance of plateau and isochron ages at the 95% confidence level, the difference in ages must be less than $1.96(\sigma_1 2 + \sigma_2 2)^{1/2}$, where σ_1 is the standard deviation of the plateau age and σ_2 the standard deviation of the isochron age (McIntyre et al., 1966). This criterion is met as the difference in the two ages is 4 m.y., which is indeed less than $1.96(\sigma_1 2 + \sigma_2 2)^{1/2} = 10.55$. Similarly, the difference (equal to 21.2) between the $^{40}Ar/^{36}Ar$ intercept value of 274.3 ± 11.4 and the atmospheric ratio of 295.5 should be less than $1.96(\sigma_1 2 + \sigma_2 2)^{1/2} = 22.3$, which is barely the case. Because all four of the criteria are satisfied, these results can be considered to yield a reliable crystallization age. A weighted mean of the plateau age and the isochron age gives a crystallization age of 110 ± 2 Ma (2σ) for basement at Site 843.

Discussion

The $^{40}Ar/^{36}Ar$ value for the intercept of the isochron (Fig. 3B) is slightly lower than the atmospheric value. Examination of the isochron diagram (Fig. 3B) shows that the intercept value is not controlled by the low-temperature increment, because the large analytical errors give it little weight in the regression. As was noted in the sample description, this sample comes from the interior of a massive flow and has only sparse vesicles. Estimates of the depth of eruption for these basalts indicate a range from 1700 to 2000 m based on the model of Sclater et al. (1971). The hydrostatic pressure in this depth range could prevent complete degassing of magmatic Ar from a massive flow that has been rapidly quenched. Plateau ages calculated assuming atmospheric $^{40}Ar/^{36}Ar$ yield younger ages if in reality there is an inherited Ar component with $^{40}Ar/^{36}Ar$ lower than the atmospheric ratio. However, because inherited mantle $^{40}Ar/^{36}Ar$ is almost certainly much greater than 300 (R. Duncan, pers. comm., 1993) and the intercept is statistically indistinguishable from the atmospheric value, inherited Ar is not considered a problem. Pringle (1992) suggested that isochron ages are preferable to weighted plateau ages, because they make no assumptions about the composition of nonradiogenic ^{40}Ar and because the error estimates include both an estimate for the experimental precision of each increment and an estimate for the scatter about the final isochron age. Nevertheless, the weighted mean of 110 ± 2 Ma (2σ) is considered to yield the best estimate of the crystallization age for the basement because it gives the best agreement with other isotopic systems in the basalts discussed next.

Measurements of the Sm–Nd and Rb–Sr systematics of basalts from Site 843, made as part of the petrochemical studies (King et al., this volume) and studies of alteration processes later in this paper, also provide information on the crystallization age of the basalts. A Sm–Nd isochron plot (Fig. 4) of three leached-rock and whole-rock pairs yields a crystallization age of 112 ± 9 Ma for Site 843 basalts. These three basalts have the same initial $^{143}Nd/^{144}Nd$ ratios at 110 Ma (within analytical precision), and differences in $^{143}Nd/^{144}Nd$ today are due to differences in $^{147}Sm/^{144}Nd$ over time. The difference between the leached-rock and whole-rock $^{143}Nd/^{144}Nd$ is assumed to be the result of selective dissolution during leaching of various mineral phases having different Sm/Nd ratios, without any incongruent dissolution effects on $^{143}Nd/^{144}Nd$ or $^{147}Sm/^{144}Nd$ in the residual mineral phases. The three pairs define lines that have essentially the same slope within the analytical errors (see inset in Fig. 4). If all the Site 843 basalts are used, the regression yields an apparent age of 131 ± 11 Ma. This age is considered unreliable based on the influence of different initial $^{143}Nd/^{144}Nd$ values attributed to slight mantle heterogeneity in the source of these basalts (King et al., this volume).

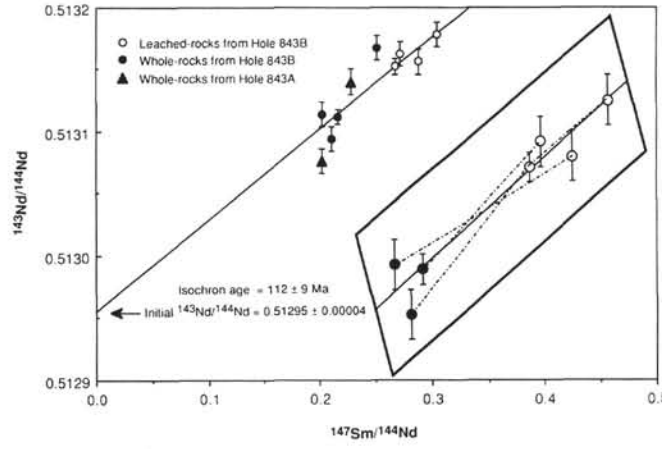

Figure 4. Sm/Nd isochron diagram for basalts from Site 843 with ±2σ analytical errors. Errors for $^{147}Sm/^{144}Nd$ are less than the size of the symbols plotted. The regression line is for just the paired whole-rock and leached-rock analyses, which are shown in more detail in the inset. The dashed and dotted lines connect the whole-rock analyses to their corresponding leached-rock analyses. Note that the slopes of the dashed and dotted lines would parallel the overall regression line if the analytical errors are taken into account. The isochron age was calculated from the slope of the line fitted by least-squares methods using the analytical uncertainties (York, 1969).

Another limit for the crystallization age of the basement comes from Rb–Sr systematics of hydrothermally altered Rb-enriched basalts from Site 843. Three of the most altered basalts show an isochronous relationship (Fig. 5) that yields an age of 112 ± 8 Ma (1σ) with an initial $^{87}Sr/^{86}Sr$ of 0.70295 ± 0.00005 (1σ), which is consistent with alteration by Cretaceous seawater (values presented later in the paper). Age bounds from the least altered basalts are more problematical, because even slight alteration of very low Rb/Sr and low $^{87}Sr/^{86}Sr$ rocks can result in either positive or negative slopes on isochron diagrams.

Three of the least altered basalts (based on the highly subjective criteria of simply having low $^{87}Sr/^{86}Sr$ for their $^{87}Rb/^{86}Sr$ and yet still covering a wide range of Rb/Sr ratios in Fig. 5) yield an apparent age of 104 ± 4 Ma (1σ) with an initial $^{87}Sr/^{86}Sr$ of 0.70260 ± 0.00002 (1σ). More will be said about the Rb–Sr systematics of the basalts later in the paper.

The Sm–Nd and Rb–Sr systematics for Site 843 basalts indicate crystallization ages in the same range as the ^{40}Ar–^{39}Ar incremental-heating experiments. A weighted mean (weighted inversely by the variance) calculated for the five best age estimates (Table 1) gives a crystallization age of 110 ± 2 Ma, consistent with the weighted mean of the ^{40}Ar–^{39}Ar incremental-heating experiment. Because of the age concordance of the three different isotopic systems (^{40}Ar–^{39}Ar, Sm–Nd, Rb–Sr) measured directly on the drilled basalts, a crystallization age of 110 ± 2 Ma for the basement at Site 843 is considered reliable. This age of 110 Ma falls at the upper end of previous age estimates (80 to 110 Ma) for oceanic crust near the Hawaiian Islands.

Shipboard paleontologic analysis of nannofossils in sediments directly overlying the basalts at Site 843 gives a late Albian to early Cenomanian zonal assignment of CC9b, which equates to an age for the lowermost sediments of 94 to 100 Ma, according to the Harland et al. (1990) time scale (Dziewonski, Wilkens, Firth, et al., 1992). Because of their depositional nature, sediments can provide only minimum estimates for the age of the basement on which they are deposited, but even so, a 10–15-m.y. hiatus represents a considerable amount (40–60 m) of missing sediment. The disagreement between the paleontologic age and the radiometric age might be explained by the following: (1) the age determined for the basement may be too old; (2) the age-dated basalts come from deeper in the crustal section

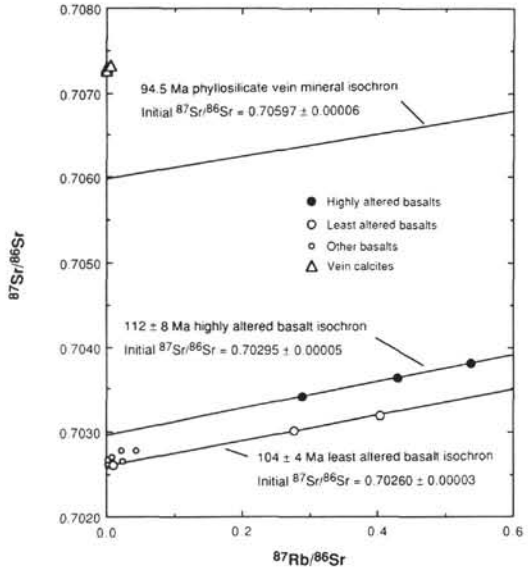

Figure 5. Rb/Sr isochron diagram for basalts and calcite veins in the basalts at Site 843. Analytical errors are less than the size of the symbols plotted. The 94.5 Ma isochron for the phyllosilicate vein minerals defined in Figure 6 is shown for reference. Three highly altered basalts define an 112 ± 8 Ma isochron whereas three of the least altered basalts define an 104 ± 4 Ma isochron. The ages defined by the basalt isochrons are consistent with the 110 ± 2 Ma age from ^{40}Ar–^{39}Ar dating. The initial $^{87}Sr/^{86}Sr$ for the 94.5 Ma phyllosilicate isochron lies between the basalts and the calcite veins, indicating equilibration with different hydrothermal solutions.

and are older than the surface flows and associated sediments; (3) the nannofossil zone (CC9b) may extend to older ages than previously recognized; (4) a hiatus exists between the youngest basalt flow and the oldest sediment on top of basement; (5) some combination of any or all of the preceding possibilities.

Possibility (1) does not seem likely because of the age concordance of the three different isotopic dating systems (^{40}Ar–^{39}Ar, Sm–Nd, Rb–Sr), which indicates the 110 Ma date is reliable. Possibility (2) cannot be adequately evaluated with the data presently available; however, a 10- to 15-m.y.-long volcanic history seems unlikely because the maximum range observed for seamounts has been 7 m.y. (Pringle et al., 1991) and is more commonly about 4 m.y. for the Hawaiian Islands. Possibility (3) also cannot be evaluated with the data presented here, but it is unlikely that nannofossil Zone CC9b can be extended back to 110 Ma (J. Firth, pers. comm., 1992). A hiatus as in possibility (4) is the most likely explanation for the difference observed for the basement and sediment ages. In the next section of this paper, on the timing of alteration events, it will be shown that the vein minerals indicate both hydrothermal activity and intrusion of seawater into basement extended until 94.5 Ma at Site 843. A thick sediment cover of 40–60 m would have accumulated by 100 Ma if uninterrupted sedimentation started at 110 Ma. Because a 50-m thickness of sediment is expected to impede the diffusive flow of seawater into the crust (Karato and Becker, 1983), it seems probable that sediments did not begin accumulating until the 94 to 100 Ma period indicated by the nannofossils. A more thorough discussion of the hiatus can be found later in this paper.

The South Hawaiian Seamount province is an ill-defined grouping of small- to medium-sized volcanoes similar to many other Cretaceous seamounts formed in the Central and Western Pacific. The greatest concentration of South Hawaiian Seamounts is found near the island of Hawaii (Fig. 1). Some of the most prominent of these seamounts form an inverted V shape and include the Cross and McCall seamounts, which have been radiometrically dated by ^{40}Ar–^{39}Ar incremental fusion techniques. Cross is located 120 km to the

Table 1. Age dates obtained for Site 843 basalts using ^{40}Ar–^{39}Ar, Sm–Nd, and Rb–Sr isotopic methods.

Method	Age (Ma)
^{40}Ar–^{39}Ar isochron	111 ± 2
^{40}Ar–^{39}Ar plateau	107 ± 5
Sm/Nd isochron leached-rock and whole-rock pairs	112 ± 9
Rb/Sr isochron altered basalts	112 ± 8
Rb/Sr isochron least altered basalts	104 ± 4
Weighted mean of all ages	110 ± 2

southeast of Site 843 and has yielded an age of 85 ± 4 Ma, whereas McCall is 210 km southeast and dated at 83 ± 0.5 Ma (Sager and Pringle, 1987). In addition, older conventional K–Ar analyses have been performed for Cross giving an age of 88 ± 2 Ma, as well as for seamount HD-1, located about 200 km to the southeast of Site 843, giving ages between 88 and 91 Ma (Dymond and Windom, 1968).

The implication of these seamount ages is that the South Hawaiian Seamount province must have been erupted 20–30 m.y. after the oceanic crust formed at the Pacific/Farallon spreading center at 110 Ma. Studies of lithospheric flexure and compensation for Cretaceous seamounts near the Hawaiian Islands suggest that these volcanic edifices were constructed in a variety of crustal settings ranging from young and weak to older and rigid (e.g., Watts et al., 1980; Schwank and Lazarewicz, 1982; Freedman and Parson, 1986). Because the seamounts were erupted well off axis, it would appear that there must have been some thermal rejuvenation of the crust during emplacement of the seamount province. A complicating factor for interpreting studies of seamount compensation, however, is that some small seamounts probably formed at the ridge crest. In particular, the petrochemistry of Hole 843A basalts (King et al., this volume), as well as the 75- to 150-m elevation of the site above the surrounding seafloor (Dziewonski, Wilkens, Firth, et al., 1992), indicate that either a small seamount or an abyssal hill was drilled at this location.

Current models of past motions of the Pacific Plate are probably not correct prior to 70 Ma. Paleomagnetic studies of the basalts indicate a paleolatitude of about 10°S (Dziewonski, Wilkens, Firth, et al., 1992; Helsley, this volume). A paleolatitude of about 24°S is predicted using the model of Engebretson et al. (1985) for absolute plate motions relative to the hot spot reference frame to backtrack Site 843 from its present location (19°20′N) to the location at 110 Ma. The 14° discrepancy in paleolatitude is significant. Furthermore, the paleolatitudes of the South Hawaiian Seamounts predicted using the model of Engebretson et al. (1985) are 15°–17°S rather than the approximately equatorial paleolatitudes found by Sager and Pringle (1987). Additional modeling is needed to satisfy the limits now imposed by the 110-Ma age of the Site 843 basalts.

IMPLICATIONS OF VEIN MINERALS FOR HYDROTHERMAL PROCESSES

Sample Description and Preparation

Vein Minerals

Shipboard descriptions of cores and thin sections from Site 843 are given by Dziewonski, Wilkens, Firth, et al. (1992). The primary vein used in this study comes from Section 136-843B-1R-3 at the intervals 20–22 cm and 25–27 cm, recovered about 18 m below the sediment/basement contact (Fig. 2) and about 3 m beneath the basalt dated by ^{40}Ar–^{39}Ar techniques. The vein is 8 mm at its widest and, as traced along the core, results from the coalescence of three smaller veins. The vein consists of an early-formed dark green celadonite, which was followed in the paragenesis by limonite, smectites, gray to dark grayish green zeolites, lighter apple-green celadonite, and calcite veinlets that crosscut all the other vein minerals. The basalt

immediately next to the vein is highly altered and darker in color than the lighter gray basalt several centimeters farther away from the vein. The groundmass of the highly altered dark gray basalt contains numerous patches of a blue-green celadonite plus other alteration phases. The light gray basalt is about 15%–20% altered, mostly due to the breakdown of olivine and glass with some slight alteration of plagioclase and clinopyroxene. Microprobe analyses of alteration phases in Site 843 cores are given by Alt (this volume).

Core samples containing the veins were initially cleaned by grinding exposed surfaces with Al grit to remove saw and drill marks, followed by repeated cleaning with deionized water in an ultrasonic bath to remove the grit. The vein material was then split from the surrounding basalt using a steel chisel and crushed in a steel mortar and pestle to a size of approximately 5 mm for the chips. The vein minerals were then picked under a binocular microscope to prepare the following concentrates of the various alteration phases: light apple-green celadonite; dark green celadonite; mixed-phase smectites and celadonites; calcite; and a whole vein fraction with only minor intergrown calcite. Each fraction was then washed several times with ultrapure quartz-distilled water and dried. Each of the fractions, with the exception of the calcite, was then coarsely ground in an agate mortar. The whole-vein fraction, without any further treatment, was dissolved using the normal procedures outlined herein. The other fractions received the following additional chemical treatments to obtain better separation of phases.

The apple-green and dark green celadonite fractions were first treated with 1N acetic acid (HOAc) for 5 min to dissolve any carbonate adhering to or intergrown with the clay phases. After several rinses with ultrapure water, the clays were next treated with 0.75N HCl for 5 min to remove labile Sr in the interlayer sites of the clay minerals (e.g., Hart and Staudigel, 1986). The clays were then rinsed several times with ultrapure water, dried, weighed after coming to equilibrium with the atmosphere, and dissolved as outlined in the "Analytical Methods" section.

The mixed-phase smectite and celadonite fraction was treated with 2N HOAc for 30 min in an ultrasonic bath to dissolve any carbonate. This treatment had the additional effect of disaggregating the clays. Due to density and possibly size differences, the clays separated into two fractions: a brown-green mixed smectite/celadonite phase and a pistachio-green mixed celadonite/smectite phase. The two fractions were washed with ultrapure water several times, dried, weighed after coming to equilibrium with the atmosphere, and dissolved as outlined in the "Analytical Methods" section.

The calcite-rich fraction was intimately intergrown with the other phases and could not be separated by hand-picking into a pure calcite separate. Therefore, 2N HOAc was used to selectively dissolve only the calcite, leaving the other alteration minerals as a residue. The supernate was separated from the residue and centrifuged to remove any clay minerals suspended in the solution. The clay minerals, however, proved difficult to completely remove from the supernate even after multiple successive centrifugation steps followed by successive dryings. After the final drying, the sample was allowed to come to equilibrium with the atmosphere and weighed. The amount of carbonate dissolved was determined by two methods: (1) loss of weight by the original mixture of calcite and phyllosilicates due to dissolution by HOAc; and (2) calculating the amount of $CaCO_3$ represented by the weight of $Ca(OOC_2H_3)_2 \cdot 0.5H_2O$ after drying. The two methods were in good agreement, with only a 0.3% difference between estimates probably related to loss of clays during the centrifugation steps. The sample was then converted to chlorides and processed using the ion-exchange procedures outlined herein.

Sample 136-843B-1R-2, 30–31 cm, was recovered about 1.5 m beneath the basalt dated by ^{40}Ar–^{39}Ar techniques and lies about 1.5 m above the previously described vein (Fig. 2). The analyzed sample comes from the calcite crystals lining the walls of a vug in the basalt. The core surface was prepared in the same manner as the previous core. In order to determine if there has been any recent exchange of Sr isotopes between the calcite crystals and seawater, a selective dissolution technique using 2N HOAc was employed to dissolve only the free surfaces of the calcite crystals. The resulting supernate was centrifuged, dried, and the weight determined using the two methods described previously, which were in perfect agreement in this case. The sample was then converted to chlorides and processed using normal ion-exchange procedures outlined herein.

Sample 136-843B-2R-2, 42–46 cm, comes from about 28 m beneath the other cores used in this study. Based on logging results (Dziewonski, Wilkens, Firth, et al., 1992; Goldberg and Moos, 1992), the core is from a zone of high permeability that might serve as a conduit for any recent fluid flow. The sample was an intergrown mixture of calcite and Al saponite (for analyses see Alt, this volume). The surface of the core was prepared using the procedures described previously; and the sample was then crushed to yield chips of about 5-mm diameter. Two fractions were handpicked using a binocular microscope: an Al saponite plus minor calcite fraction and a pure sparry calcite fraction without any inclusions or discoloration. The Al saponite fraction was coarsely ground in an agate mortar and treated with 2N HOAc to dissolve the minor calcite. The Al saponite fraction was next washed four times using ultrapure water with centrifugation between washes. The resulting carbonate-free material was then dried, weighed and processed as outlined in the "Analytical Methods" section. The calcite fraction was washed with ultrapure water several times, dried, weighed and then dissolved in 6N HCl and processed using normal ion-exchange procedures outlined herein.

Carbonate Sediments

Core 136-843A-3R-1 recovered the contact between the sediments and the basalt (Dziewonski, Wilkens, Firth, et al., 1992). The sediments recovered in the upper part of the core (0–76 cm) are primarily a wavy, laminated, brown nannofossil limestone. This limestone is composed principally of silt- to clay-size rhombs of calcite and nannofossils, along with minor detrital silicate clays (1%–10%). In the lower part of the core just above basement (77–84 cm interval), a laminated brown and reddish-yellow nannofossil calcareous clay with parallel laminations was recovered. To determine the $^{87}Sr/^{86}Sr$ of seawater at the time of basalt alteration, Sr isotopes were measured on carbonate fractions separated from the nannofossil limestone (8–10 cm and 74–76 cm intervals). The time difference between these two intervals is 90 to 150 thousand years based on average sedimentation rates ranging from 4 to 7 m/m.y. for similar sites in the Pacific (e.g., Lancelot and Larson, 1975).

The surfaces of the consolidated core samples were rinsed several times with deionized water to remove any adhering extraneous material. The samples were broken into small pieces and dried in an oven set at 60°–70°C for 24 hr. Two experiments were conducted to establish whether recrystallization and cementation of the nannofossil ooze had any effect on the $^{87}Sr/^{86}Sr$ of the limestone. In the first experiment, a 0.2-g piece of the whole limestone from the 74–76 cm interval was reacted with 1N HOAc for 5 min, and the supernate was decanted, centrifuged to remove clays, dried, and processed as outlined in the "Analytical Methods" section. In the second experiment, the mixture of nannofossils and clays remaining from the first experiment was further treated with 1N HOAc to dissolve cement adhering to nannofossil surfaces. The sample was then washed a number of times to remove clay-sized material. The final concentrate consisted mainly of large nannofossils and calcite rhombs, with a minor amount of silicate clay minerals (≤2% by weight) probably residing in the interiors of the nannofossils. The concentrated carbonate was then completely dissolved in 2N HOAc and the minor insoluble clay residue removed by centrifugation. The supernate was then dried and processed as outlined in the "Analytical Methods" section.

A similar carbonate concentrate was prepared from the 8–10 cm interval limestone. This concentrate consisted mainly of broken fragments of the nannofossils, rhombs of calcite and a minor fraction of

Table 2. Sr and Nd isotope ratios and trace element abundances of alteration phases and basalts at Site 843.

Core, section, interval (cm)	$^{87}Sr/^{86}Sr$	± 2SE	$^{143}Nd/^{144}Nd$	± 2SE	$^{87}Rb/^{86}Sr$	± 2SE	$^{147}Sm/^{144}Nd$	± 2SE	Rb (ppm)	Sr (ppm)	Sm (ppm)	Nd (ppm)
Vein minerals												
136-843B-1R-3, 20-27												
Light apple green	0.97310	4	0.513152	12	198.74	0.85	0.1930	0.0010	148.5	2.22	0.1327	0.4157
Dark green	0.88027	2	0.513113	18	129.51	0.85	0.1951	0.0010	146.6	3.33	0.1305	0.4045
Pistachio	0.79243	4	0.513150	10	70.26	1.13	0.1773	0.0010	152.9	6.35	0.1636	0.5592
Brown green	0.75270	2	0.513149	10	34.77	0.14	0.1900	0.0010	115.9	9.69	0.5854	1.862
Whole vein	0.71907	4	0.513147	10	8.32	0.22	0.1886	0.0010	120.5	41.96	0.3074	0.9852
Calcite	0.70732	2	0.513077	10	0.0067	0.0001	0.1470	0.0006	0.28	121.2	0.8495	3.492
136-843B-2R-2, 42-46												
Al saponite	0.70793	3			1.4714	0.0052			6.27	12.32		
Calcite	0.70730	2			0.0001	0.0000			0.004	86.94		
136-843B-1R-2, 30-31												
Calcite	0.70725	2	0.513070	14	0.0009	0.0001	0.1654	0.0010	0.014	46.36	0.1721	0.6288
Basalts												
136-843A-3R-2, 10-12 (WR)	0.70278	1	0.513076	10	0.0213	0.0001	0.2020	0.0004	1.06	143.8	3.653	10.93
136-843A-3R-2, 10-12 (LR)	0.70261	2			0.0102	0.0001			0.62	175.4		
136-843A-3R-2, 38-40 (WR)	0.70302	2	0.513140	10	0.2756	0.0010	0.2282	0.0004	13.97	146.6	2.527	6.692
136-843B-1R-1, 15-17 (WR)	0.70281	2	0.513094	10	0.0315	0.0001	0.2104	0.0004	1.41	129.4	3.455	9.928
136-843B-1R-1, 15-17 (LR)	0.70264	2	0.513178	10	0.0020	0.0001	0.3049	0.0004	0.07	102.1	1.297	2.570
136-843B-1R-1, 15-17 (LR)	0.70265	1	0.513152	06	0.0236	0.0001	0.2672	0.0004	1.11	135.4	1.701	3.847
136-843B-1R-1, 61-63 (WR)	0.70268	1	0.513167	10	0.0027	0.0001	0.2514	0.0004	0.12	129.9	2.007	4.826
136-843B-1R-1, 61-63 (LR)	0.70262	2			0.0014	0.0001			0.06	122.4		
136-843B-1R-3, 25-27 (WR)	0.70381	2	0.513092	10	0.5366	0.0015	0.2021	0.0004	22.40	120.7	3.774	11.29
136-843B-1R-4, 49-51 (WR)	0.70319	2	0.513177	10	0.4034	0.0006	0.2746	0.0004	17.15	123.0	1.514	3.332
136-843B-4R-3, 29-31 (WR)	0.70341	2	0.513112	06	0.2889	0.0008	0.2161	0.0004	11.37	113.8	3.021	8.450
136-843B-4R-3, 29-31 (LR)	0.70279	2	0.513162	10	0.0433	0.0001	0.2722	0.0004	1.89	126.4	2.114	4.696
136-843B-2R-2, 77-79 (WR)	0.70364	1	0.513114	10	0.4285	0.0009	0.2024	0.0004	18.55	125.2	3.732	11.14
136-843B-2R-2, 77-79 (LR)	0.70270	2	0.513156	10	0.0076	0.0001	0.2877	0.0004	0.37	141.8	2.257	4.742

Notes: Nd isotopes were analyzed as oxides, and the isotopic fractionation correction applied was $^{148}NdO/^{144}NdO = 0.242436$ ($^{148}Nd/^{144}Nd = 0.241572$). The fractionation correction used for Sr was $^{86}Sr/^{88}Sr = 0.1194$. Nd isotopic data are reported relative to the measured $^{143}Nd/^{144}Nd$ values for the La Jolla Nd standard of 0.511855 ± 0.000012 total range. Sr isotopic data are reported relative to a $^{87}Sr/^{86}Sr$ value of 0.71022 for NBS 987; the measured $^{87}Sr/^{86}Sr$ for NBS 987 during the tenure of this study was 0.71021 ± 0.00002 total range. Total procedural blanks are less than 20 pg for Nd and Sm, less than 10 pg Rb, and less than 200 pg for Sr; all blanks are negligible for these analyses. 2SE = two standard errors; for Sr and Nd isotopes the errors are reported relative to the last digit(s). WR = whole-rock analysis; LR = leached-rock analysis (leached following the method of Mahoney, 1987).

adhering clay minerals (~2% by weight). The carbonate material was dissolved with 2N HOAc, the clays were removed by centrifugation, the supernate was dried and then processed as outlined in the "Analytical Methods" section.

Basalts

Isotopic and trace element analyses were performed as part of the petrochemical study of basalts from Site 843, and the details of sample preparation and leaching techniques are given by King et al. (this volume). In addition, two more basalts were analyzed for Sr and Nd isotope systematics following the same techniques. The first sample is a very highly altered basalt from Sample 136-843B-1R-3, 25–27 cm, that forms the wall of the major vein described previously in the "Vein Minerals" section. The second basalt is Sample 136-843B-1R-4, 49–51 cm, which has a very high Rb/Sr ratio but is otherwise lacking petrographic or geochemical evidence for a significant degree of alteration (King et al., this volume).

Analytical Methods

Isotopic ratios of Sr and Nd, as well as isotope dilution abundances of Rb, Sr, Sm, and Nd (Tables 2 and 3) were measured in the Isotope Laboratory at the University of Hawaii, using slightly modified methods of Mahoney et al. (1991). Silicate minerals were digested with a 2:1 HF-HNO_3 mixture, and carbonates were dissolved with either acetic acid (HOAc) or HCl depending on whether clay minerals were also present. After conversion to chlorides, samples were spiked with ^{87}Rb, ^{84}Sr, ^{149}Sm, and ^{146}Nd tracers. Rb and Sr were eluted using 2N HCl on pressurized cation exchange columns, and then the rare earth elements (REE) were eluted as a group using 4N HCl. Sm and Nd were separated from the other REE with α hydroxy-isobutyric acid elution (e.g., Lugmair et al., 1975). Total procedural blanks are less than 20 pg for Nd and Sm, less than 10 pg for Rb, and less than 200 pg for Sr; all blanks are negligible for these analyses.

Table 3. Sr and Nd isotope ratios and trace element abundances of carbonate sediments immediately above basement at Site 843.

Core, section, interval (cm)	$^{87}Sr/^{86}Sr$	± 2SE	Rb (ppm)	Sr (ppm)	$^{87}Rb/^{86}Sr$
136-843A-3R-2, 8-10					
Nannofossils	0.70733	3	0.489	116.2	0.0122
Nannofossils	0.70736	2			
Nannofossils	0.70734	2			
Weighted mean	0.70734	1			
136-843A-3R-2, 74-76					
Nannofossils	0.70735	3	0.197	235.4	0.0024
Nannofossils	0.70735	2			
Nannofossils	0.70735	2			
Weighted mean	0.70735	1			
136-843A-3R-2, 74-76					
Cement	0.70734	1	0.0825	849.2	0.0003
Weighted mean of all fractions	0.70734	1			

	$^{143}Nd/^{144}Nd$	± 2SE	Sm (ppm)	Nd (ppm)	$^{147}Sm/^{144}Nd$	$^{143}Nd/^{144}Ndi$
136-843A-3R-2,74-76						
Nannofossils	0.512399	10	1.992	10.49	0.1148	0.51233
Cement	0.512426	10	1.969	10.22	0.1164	0.51235

Notes: 2SE = two standard errors; for Sr and Nd isotopes the errors are reported relative to the last digit(s). $^{87}Sr/^{86}Sr$ ratios for the nannofossils were measured on the same sample split. $^{143}Nd/^{144}Ndi$ = initial ratio at 95 Ma. Analytical details are given in the footnote to Table 2.

Mass spectrometric measurements were performed on the VG Sector multicollector instrument at the University of Hawaii. Because of the limited size of some prepared sample fractions (20–100 mg) and the low Sr abundances in celadonites and smectites (2–12 ppm), Sr yields after the chemical separations were usually between 20 and 100 ng. Sr isotopic analyses on such small samples were made using

single tungsten filaments with a TaF activator solution that improves the stability and efficiency of Sr ionization (Birck and Allègre, 1978; Birck, 1986). For samples with higher Sr abundances, 600–800 ng of Sr was loaded onto a single Ta filament with a Ta_2O_5 substrate (e.g., Birck, 1986). Between 10 and 150 ng of Nd was loaded onto a single Re filament and then oxidized (e.g., Lugmair et al., 1975).

Normalization values and measured ratios for Nd- and Sr-isotopic standards are given in the footnotes to Tables 2 and 3. Decay constants used are those of Steiger and Jäger (1977).

Results

Analyses of the six phyllosilicate vein mineral fractions and the three carbonate vein mineral fractions for $^{87}Sr/^{86}Sr$, $^{143}Nd/^{144}Nd$, and Rb, Sr, Sm, and Nd abundances are presented in Table 2 along with analyses of Site 843 basalts. Analyses of the two nannofossil fractions and the carbonate cement from the limestone unit directly above the igneous basement are presented in Table 3.

The Rb and Sr contents of the celadonites and smectites are similar to those reported by other researchers working on similar alteration phases (e.g., Hart and Staudigel, 1986). These phases provide a large range in $^{87}Rb/^{86}Sr$ (1.5 to 200), which is ideal for high-precision Rb/Sr isochron dating (Fig. 6). The celadonites and smectites contain low, but significant amounts of Sm and Nd (Table 2). The REE contents of these phases are greater than would be expected in minerals precipitated from seawater-dominated hydrothermal fluids with respective Sm and Nd contents of about 0.2×10^{-9} and 1.1×10^{-9} g/g, (Michard et al., 1983). The Sm contents of the phyllosilicates are similar to those reported by Tlig (1982) for smectites from veins in Hole 417A basalts. The $^{147}Sm/^{144}Nd$ and $^{143}Nd/^{144}Nd$ of the phyllosilicate vein minerals are similar to those in Site 843 basalts, suggesting that the basalt-derived component dominates the REE content of the hydrothermal fluids from which these minerals precipitated.

The Rb and Sr contents of calcites from veins in Site 843 basalts (referred to hereafter as vein calcites) are similar to values found for other vein calcites in the oceanic crust (e.g., Hart and Staudigel, 1986). There is a general correlation between $^{87}Sr/^{86}Sr$ ratios and Sr contents of the calcites, that has been observed in similar studies (e.g., Staudigel et al., 1981). As the Sr contents of the calcites increase, their $^{87}Sr/^{86}Sr$ ratios approach values for contemporaneous seawater as recorded by the overlying carbonate sediments (Table 3 and Fig. 7). Sm and Nd contents and $^{143}Nd/^{144}Nd$ ratios, on the other hand, reflect a predominantly basaltic component for the REE content of the hydrothermal fluids from which the calcites precipitated (Fig. 8).

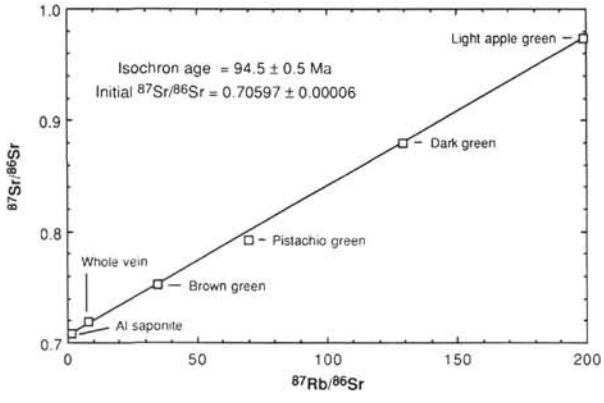

Figure 6. Rb/Sr isochron diagram for the six phyllosilicate vein mineral fractions from Hole 843B. Analytical uncertainties are slightly less than the size of the symbols plotted. The 94.5 ± 0.5 Ma isochron age was calculated from the slope of the line fitted by the least-squares methods using the analytical uncertainties (York, 1969). The pistachio-green fraction shows the largest departure from the isochron; however, exclusion of it from the regression has an insignificant effect.

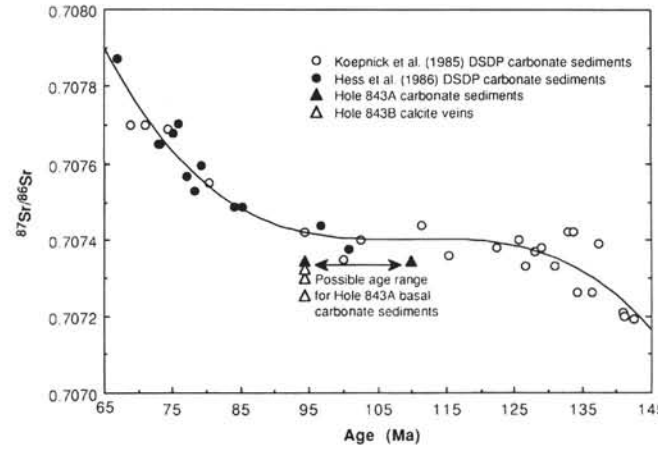

Figure 7. Comparison among the Cretaceous seawater $^{87}Sr/^{86}Sr$ evolution curve, carbonate sediments immediately above basement in Hole 843A, and calcite veins in Hole 843B basalts. The seawater evolution curve is based on open-ocean carbonate samples with minimal diagenetic changes and thus differs from other seawater evolution curves that include data from continental areas (e.g., Koepnick et al., 1985). The arrows show the allowable age range for Hole 843A carbonate sediments based on a basement age of 110 Ma and the minimum age of 94 Ma for nannofossils in the basal sediments. The seawater evolution curve is essentially flat during the time period from 94 to 125 Ma.

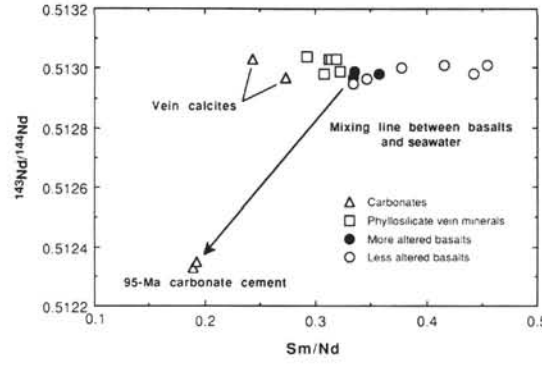

Figure 8. Plot of $^{143}Nd/^{144}Nd$ against Sm/Nd at 95 Ma for basalts, phyllosilicate vein minerals, and vein calcites from Holes 843A and 843B. The arrow is a mixing line between the basalts and 95-Ma seawater, which is represented by the carbonate cement in the limestone just above basement in Hole 843A. Neither the vein calcites or the phyllosilicate vein minerals fall along the mixing trend, but instead indicate these minerals precipitated from fluids derived from the alteration of the basalts.

A Rb/Sr isochron diagram for the six phyllosilicate vein mineral fractions is shown in Figure 6. The alteration mineral fractions define an isochron for which a York-type regression with correlated errors (York, 1969) yields an age of 94.5 ± 0.5 Ma (2σ) with an initial $^{87}Sr/^{86}Sr$ ratio of 0.70597 ± 0.00006 (2σ). The isochron records the last equilibration of these minerals with a hydrothermal fluid at about 16 m.y. after the formation of the igneous basement at 110 Ma. The pistachio green celadonite/smectite mixture and the whole-vein sample show slight deviations from the isochron; however, because of the large influence of the light green and Al saponite fractions on the slope and intercept, exclusion of these fractions from the regression does not result in any significant changes in either the age (94.6 ± 0.5 Ma) or the initial $^{87}Sr/^{86}Sr$ ratio (0.70595 ± 0.00006).

The relationships between the phyllosilicate vein mineral isochron and the vein calcites, as well as the basalts, are shown in Figure 5. The vein calcites have $^{87}Sr/^{86}Sr$ greater than the initial $^{87}Sr/^{86}Sr$ (0.70597) for the phyllosilicate vein minerals, indicating that the

calcites did not precipitate from the same solutions as the celadonites and smectites. This is consistent with previous studies of vein carbonates, which have shown that they are generally late-stage precipitates with $^{87}Sr/^{86}Sr$ approaching seawater compositions (e.g., Hart and Staudigel, 1986). The crosscutting nature of the calcite veinlets in Core 136-843B-1R-3 also clearly demonstrates the later paragenesis of these veins when compared with celadonites and smectites.

Basalts from Site 843 all have $^{87}Sr/^{86}Sr$ less than the initial $^{87}Sr/^{86}Sr$ for the phyllosilicate vein minerals (0.70597) and plot well below the isochron for the alteration phases (Fig. 5). The three most petrographically and geochemically altered basalts, Samples 136-843B-1R-3, 25–27 cm, 136-843B-2R-2, 77–79 cm, and 136-843B-4R-3, 29–31 cm, define an isochron with an age of 112 ± 8 Ma (1σ) and initial $^{87}Sr/^{86}Sr$ of 0.70295 ± 0.00005 (Fig. 5). The initial $^{87}Sr/^{86}Sr$ is typical of many altered basalts recovered by drilling. The three least-altered basalts are: Samples 136-843A-3R-2, 10–12 cm (leached), 136-843A-3R-2, 38–40 cm, and 136-843B-1R-4, 49–51 cm, based on the subjective criteria of simply having a low $^{87}Sr/^{86}Sr$ for their $^{87}Rb/^{86}Sr$ (Fig. 5). These three basalts define an isochron with an age of 104 ± 4 Ma (1σ) and an initial $^{87}Sr/^{86}Sr$ of 0.70260 ± 0.00002.

The $^{87}Sr/^{86}Sr$ of seawater contemporaneous with the formation of the alteration phases has been established using the nannofossil concentrates from Samples 136-843A-3R-2, 8–10 cm, and 74–76 cm, and the carbonate cement leached from the 74–76 cm interval (Table 3). Based on replicate $^{87}Sr/^{86}Sr$ analyses, there is no statistical difference between the nannofossils from these two intervals deposited 90 to 150 thousand years apart or between the nannofossils and the carbonate cement. The weighted mean of all the $^{87}Sr/^{86}Sr$ analyses is 0.70734 ± 0.00001 (2σ), which is taken to be the value for seawater at 95 Ma. The Rb/Sr ratios in the carbonates are low enough that no corrections for radioactive decay of Rb need to be made to the $^{87}Sr/^{86}Sr$ ratios. A comparison between the Site 843 value for $^{87}Sr/^{86}Sr$ in seawater and results from other studies of the evolution of $^{87}Sr/^{86}Sr$ in seawater during the Cretaceous is shown in Figure 7. The $^{87}Sr/^{86}Sr$ evolution curve for seawater appears to be essentially flat during the period from 95 to 125 Ma, based on carbonate samples from Deep Sea Drilling Project (DSDP) cores. The $^{87}Sr/^{86}Sr$ ratio measured in Site 843 nannofossils is therefore used as the value of seawater during the time period from eruption of the igneous basement at 110 Ma until closure of the hydrothermal system at 94.5 Ma.

The average $^{143}Nd/^{144}Nd$ of the carbonate cement and nannofossils from Sample 136-843A-3R-2, 74–76, when corrected to the initial value at 95 Ma, is 0.51234 (Table 3), which is taken to be the $^{143}Nd/^{144}Nd$ value for local seawater during the 95–110 Ma time interval. Direct measurements of $^{143}Nd/^{144}Nd$ in modern Pacific seawater average about 0.51249; however, there are strong vertical and horizontal gradients, and the overall range is from 0.51264 to 0.51222 (Piepgras and Wasserburg, 1980, 1982; Piepgras and Jacobsen, 1988). A $^{143}Nd/^{144}Nd$ value of 0.51234 for 95 Ma seawater is generally consistent with the results of Chyi et al. (1984), which show that ferromanganese and chert deposits in the Franciscan Assemblage record $^{143}Nd/^{144}Nd$ values for 158 Ma seawater that range from 0.51243 to 0.51238. A value of 0.51234 is also consistent with the Staudigel et al. (1985) study of fish teeth from cores taken in the Pacific, which found a $^{143}Nd/^{144}Nd$ range from 0.51233 to 0.51260 for sediments with ages between 54 Ma and 6 Ma. The $^{147}Sm/^{144}Nd$ ratio of 0.116 for the carbonate cement is also the same as the average value in modern Pacific seawater of 0.115 (Piepgras and Wasserburg, 1980).

Considerable evidence exists for solution and reprecipitation of the carbonate in this core. In particular, the Sr contents of the nannofossil separates (235 and 116 ppm) are considerably less than the Sr contents of unrecrystallized biogenic carbonates (1200–2000 ppm; e.g., Richter and DePaolo, 1988; Koepnick et al. 1985). In addition, the mere presence of the carbonate cement and its relatively high Sr content (849 ppm) are indicators of solution and reprecipitation. Richter and DePaolo (1987, 1988) demonstrated that diagenesis of extensive carbonate sections can result in decreases in $^{87}Sr/^{86}Sr$ for the bulk carbonate of up to 0.00006 in the upper portions of a section relative to contemporaneous seawater values. However, no corrections need to be made to the $^{87}Sr/^{86}Sr$ measured in this study for the following reasons: (1) the carbonate material comes from just above basement (10–70 cm), and hence there was little advection of pore water from deeper in the section due to compaction of sediments; (2) the carbonates were deposited during a long period of nearly constant seawater $^{87}Sr/^{86}Sr$ so there would be little change in pore water $^{87}Sr/^{86}Sr$; and (3) no statistical differences in $^{87}Sr/^{86}Sr$ were found between the nannofossils from the two intervals or between the nannofossils and the carbonate cement, as would be expected if diagenesis had modified $^{87}Sr/^{86}Sr$ ratios.

Discussion

Age Significance

The 94.5 ± 0.5 Ma isochron age for the phyllosilicate vein minerals is principally defined by the high Rb/Sr celadonite and mixed-layer celadonite/smectite phases (Fig. 6). This age for formation of the celadonites is considerably less than the 110 ± 2 Ma age determined for the crystallization of the basalts. Celadonites take up alkalis for a considerable time while in contact with seawater (Elderfield, 1976) and remain "open" with respect to their Rb/Sr isotope systematics until seawater circulation stops (Hart and Staudigel, 1986). The ages recorded by a particular set of alteration minerals is the "closure" age for the particular minerals involved. These ages do not necessarily record either the times of most active fluid circulation in the crust or the time of cessation of all circulation (Hart and Staudigel, 1986). Circulation of low-temperature fluids that are not involved in alteration mineral formation could conceivably continue throughout the lifetime of the crust (Hart and Staudigel, 1986).

The "open system" interpretation is supported by the observation that carbonate veins have precipitation ages in the same range as the isochron ages, even though petrographic evidence shows that carbonate precipitation usually postdates celadonite formation (e.g., Staudigel and Hart, 1985). The calcites from Site 843 form multiple generations of late crosscutting veins and have $^{87}Sr/^{86}Sr$ approaching the value for seawater at 95 Ma (Fig. 7). Although the data for seawater $^{87}Sr/^{86}Sr$ in the appropriate age range on Figure 7 is sparse, it appears unlikely that the vein calcites could precipitate from seawater-dominated fluids much later than 90 Ma, and they are more likely to be about the same age as the phyllosilicates. Because the calcites must be younger than the celadonites they crosscut, their age is fixed at about 94.5 Ma.

The phyllosilicate vein studied here has two types of celadonite: a dark green variety and a light apple-green variety that occurs later in the paragenesis. The alteration minerals formed as sequentially zoned fracture fillings from dark green celadonite at the walls to Fe oxyhydroxides to saponite at the center, with refracturing and crosscutting by later light apple-green celadonite and/or calcite. The minerals suggest a definite sequence of mineral formation, yet the dark green and light apple-green celadonites, brown-green smectite, and Al saponite all plot on the same 94.5-Ma isochron with little deviation (Fig. 6). Their conformity suggests that the minerals all reached final equilibrium with the same hydrothermal fluid and have behaved as closed systems since that time.

Not all the minerals have behaved as closed systems. The pistachio green mixed-phase celadonite/smectite deviates slightly from the 94.5-Ma isochron by plotting below it (Fig. 6). This deviation indicates several possibilities: equilibration with a different hydrothermal fluid from the other phases or open system behavior with either more recent addition of Rb or loss of radiogenic ^{87}Sr from the crystal lattice. The whole-vein fraction also deviates from the isochron, but in this case by being displaced above it (Fig. 6). Some, but not all, of the departure is explained by the inclusion of calcite in the sample. If a mixing line is drawn connecting the whole-vein sample and the intimately associated vein calcite, however, it will not inter-

sect the 94.5-Ma isochron on the Rb/Sr isochron diagram (i.e., the intersection occurs at negative $^{87}Rb/^{86}Sr$). The deviation of this mixing line away from the 94.5-Ma isochron suggests that an additional process such as loss of Rb or equilibration with a different hydrothermal fluid has affected some phase included in the vein.

On the basis of petrographic observations, some celadonites are formed early in the alteration history of the oceanic crust (e.g., Bass, 1976; Donnelly, Francheteau, et al., 1979; Alt et al., 1986; Gillis and Robinson, 1990). One of the most altered Site 843 basalts comes from immediately next to the 94.5-Ma vein and contains extensive patches of blue-green celadonite in the groundmass, yet it still falls on the 112 ± 8 Ma isochron that is consistent with the crystallization age of 110 ± 2 Ma. These highly altered basalts evidently record an early stage of alteration that occurs at the ridge crest, in which early-formed smectites replace basaltic mesostasis and are in turn replaced by celadonite (Scheidegger and Stakes, 1980; Stakes and Scheidegger, 1981). Because the celadonites in the veins remained "open" with respect to their Rb–Sr isotope systematics until most seawater circulation stopped at 94.5 Ma, the basalts must have become isolated from further interaction with hydrothermal fluids fairly soon after the initial alteration to preserve the record of this early alteration event. One possible reason for these basalts remaining isolated from further hydrothermal alteration is their low vesicularity.

The question arises about what event is recorded by the 94.5-Ma age. The vein calcites suggest that this event represents the last incursion of large volumes of seawater into the oceanic crust. One possibility for explaining this age is the effective sealing of the crust by a sufficient thickness of sediments to impede free circulation of seawater into the crust. Karato and Becker (1983) suggested that 50 m of sediment has sufficient hydraulic impedance to halt the diffusive flow of seawater into and out of the underlying crust. Beginning about 95 Ma, the crust at Site 843 entered the equatorial zone of high productivity where sedimentation rates can approach 25 m/m.y. (e.g., Lancelot and Larson, 1975). Rapid sedimentation of calcareous and siliceous oozes could therefore rapidly halt circulation within a few million years of the basement entering the equatorial zone. The biostratigraphy of the lowermost calcareous sediments is consistent with sedimentation beginning anywhere between 100 and 94 Ma. When the large differences in sedimentation rates in the oceans are taken into account, it is remarkable that previous studies of both Rb–Sr and K–Ar systematics of alteration minerals in DSDP cores have shown a similar duration for hydrothermal circulation of 10–20 m.y. after crust formation (e.g., Hart and Staudigel, 1978, 1979; Richardson et al., 1980; Staudigel et al., 1981, Staudigel and Hart, 1985; Duncan et al., 1984; Peterson et al., 1986).

There are exceptions to the general picture of a 10- to 20-m.y. limit on hydrothermal circulation in the crust. Gallahan and Duncan (1991) found that K–Ar systematics of alteration phases in the Troodos ophiolite indicate up to 30 m.y. of hydrothermal circulation in the oceanic crust. Hart and Staudigel (1986) found that off-axis intrusions of massive sill and flow complexes are recorded in the Rb–Sr isotope systematics of vein minerals in the oceanic crust. The effects of off-axis volcanism on the Rb–Sr systematics may be due to either local-scale thermally driven convection around the sills or renewed seawater hydrothermal circulation induced by the erosion of sediments during uplift caused by the emplacement of the intrusions. Therefore, it is interesting that Lindwall (1991) found high-velocity laminations in the oceanic crust beneath Site 843 that can be interpreted to represent either ultramafic sills or cumulates formed during off-axis volcanism. A possible source for these intrusions is Powers Seamount, located immediately to the east of Site 843 (Fig. 1). Although Powers Seamount has not been dated, it probably formed at the same time as the other South Hawaiian Seamounts, which have emplacement ages that range from 83 to 91 Ma (Sager and Pringle, 1987). Because the volcanism that formed the South Hawaiian Seamounts is too young to explain the 94.5-Ma event recorded by the alteration minerals, the most likely explanation for the event remains the cessation of seawater-dominated hydrothermal circulation in the ocean crust caused by sediment accumulation.

Why were no sediments accumulating before the 100 to 94 Ma period if volcanism ceased at 110 Ma? Site 843 is located on the side of a small abyssal hill or seamount that is presently 75 to 150 m above the surrounding seafloor (Dziewonski, Wilkens, Firth, et al., 1992). The most likely possibility is that the sloping topography in conjunction with scouring by bottom currents and/or slumping (e.g., Johnson, 1972) prevented the accumulation of sediments until high sedimentation rates began in the equatorial zone. An alternative possibility is that sediments did accumulate from 110 to 95 Ma, but were subsequently removed by erosion due to a process such as enhanced circulation of bottom waters (Johnson, 1972). Removal of the sediments can produce a renewed pulse of hydrothermal circulation of seawater, as suggested by LeHuray and Johnson (1989) for Site 642 in the Norwegian Sea. Regardless of whether the sediments were thin due to nondeposition or to erosion, the most probable cause of the cessation of seawater-dominated hydrothermal circulation is the accumulation of a sufficiently thick sediment cover to impede the diffusive flow of seawater into and out of the oceanic crust.

Implications for Models of Crustal Aging

The age dates derived from the phyllosilicate vein minerals and vein carbonates limit the chemically active phase of hydrothermal circulation at Site 843 to about 16 m.y. in duration. The $^{87}Sr/^{86}Sr$ of the vein carbonates suggest formation from seawater-dominated solutions no younger than 94 Ma, based on the seawater $^{87}Sr/^{86}Sr$ curve (Fig. 7) and the minimum biostratigraphic age for the basal sediment (Dziewonski, Wilkens, Firth, et al., 1992). These results have important implications for sealing of the crust to more recent incursions by seawater and precipitation of hydrothermal minerals in cracks.

The Hawaiian Arch has been uplifted about 1.4 km during the last 5 m.y. as the crust flexed due to the load imposed by construction of the islands from Kauai to Hawaii. Brocher and ten Brink (1987) showed that extensional strains imposed by this uplift resulted in the opening of cracks in Layer 2 of the oceanic crust. If filling of cracks were the only impediment to fluid flow in the crust (e.g., Anderson et al., 1977), new cracks would be expected to provide new pathways for fluid migration. However, the strong thermal gradients that are the major driving force for hydrothermally driven circulation are absent in the 110-Ma crust (e.g., Sclater et al., 1971). What does the absence of any evidence for chemically reactive fluids after 94 Ma mean for the crust at Site 843? It suggests that once the crust is effectively sealed to the free exchange of seawater by accumulation of sediment, the seal can be maintained even when subjected to a large-scale tectonic event such as the broad uplift of the Hawaiian Arch. If any fluid flow was mobilized by the uplift, it was either not chemically reactive with the vein minerals studied or followed pathways that did not intersect these veins. The Site 843 results differ from studies at Troodos where tectonism associated with the emplacement of the ophiolite was recorded by late-stage hydrothermal vein minerals (Staudigel and Gillis, 1990).

The age of precipitation of hydrothermal minerals in cracks in the crust has direct bearing on many of the unanswered questions concerning the proposed increase of seismic velocities in Layer 2A with crustal age. One of the major questions is whether seismic velocities do in fact increase beyond the 10–20 m.y. chemically active stage of hydrothermal circulation to the 40–70 m.y. age of the crust when Layer 2A appears to merge with Layer 2B (Ewing and Houtz, 1979). Jacobson (1992) reviewed the question of increased Layer 2A velocities with crustal age and suggested that there is evidence for a general increase with age, but conclusive proof is lacking because there have been no appropriate seismic lines or drilling transects along crustal flow lines away from ridges. Jacobson's compilation of available

high-resolution determinations of Layer 2A velocities vs. crustal age (fig. 3 of Jacobson, 1992) suggests that most of the increase occurs within the first 6 m.y. after crust formation. This result agrees with the studies of vein mineral ages that all fall within a time frame of 10–20 m.y. after crust formation. If Layer 2A velocities do in fact increase beyond 20 m.y., the implication of the vein mineral ages is that any velocity increase must be due to processes other than the precipitation of the alteration minerals found in the larger veins studied thus far.

One of the problems not addressed by this study or any of the others is the age systematics of vein minerals inside low-aspect-ratio cracks. These small cracks are expected to become filled relatively quickly, and as a consequence, seismic velocities increase rapidly during the early alteration history of the crust (Wilkens et al., 1991). However, because small cracks are generated throughout the cooling and tectonic history of the crust (Lister, 1977), there may be many generations of filled cracks, some of which could record in their Rb–Sr systematics alteration ages extending beyond 20 m.y. Because of the analytical limitations imposed by extremely small sample sizes for determining ages by Rb–Sr techniques, these cracks have not yet been examined. Studies up to now have focused on large veins from which mineral separates of a sufficient size and purity for analysis are easily separated. If there are increases in Layer 2A velocities beyond 20 m.y., the chemical evidence for this change will probably come from studies of low aspect ratio cracks created and filled 20 m.y. after crust formation.

Chemistry of Vein Minerals and Their Implications for Hydrothermal Fluids

Sampling of high-temperature hydrothermal fluids venting at ridge crests provides direct limits on seawater-oceanic crust interaction at elevated temperatures (e.g., Edmond et al., 1979; Michard et al., 1983; Von Damm et al., 1985). Undisturbed low-temperature fluids circulating in the basalts are not sampled as easily, and their compositions have to be inferred from either pore fluids in sediments above basement (e.g., Lawrence et al. 1975; Lawrence and Gieskes, 1981; Mottl, Lawrence, and Keigwin, 1983) or, in rare instances, from fluids collected in the basement but with drilling-induced changes in their composition (e.g., Hart and Mottl, 1983; Mottl, Anderson, et al., 1983). The alteration phases precipitated from hydrothermal fluids also provide bounds on fluid chemistry. In particular, studies of Sr and Nd isotopes as well as trace element abundances provide powerful tools for measuring water/rock ratios and identifying the sources of the fluids.

The initial $^{87}Sr/^{86}Sr$ for the phyllosilicate alteration phases is 0.70597, which is similar to the $^{87}Sr/^{86}Sr$ ratios of 0.7054–0.7059 measured for other celadonite/smectite isochrons from oceanic basalts (e.g., Hart and Staudigel, 1986). The water/rock weight ratio calculated using 0.70597 is 40, assuming the basalt end member has a $^{87}Sr/^{86}Sr$ of 0.70260 and 125-ppm Sr, whereas the seawater end member has a $^{87}Sr/^{86}Sr$ of 0.70734 and 8-ppm Sr. A water/rock weight ratio of about 40 is characteristic of the seawater zone of alteration in the oceanic crust (Gillis and Robinson, 1990). The most highly altered basalt at Site 843 (with an initial $^{87}Sr/^{86}Sr$ of 0.70295) has a water/rock weight ratio of 1.25, more typical of the low-temperature zone of alteration (Gillis and Robinson, 1990). The vein calcites, on the other hand, have water/rock weight ratios from 800 to 1800 based on their range of $^{87}Sr/^{86}Sr$ ratios. The hydrothermal fluids that precipitated the celadonites and smectites therefore had a water/rock ratio intermediate between that of the hydrothermal system that initially altered the basalts and the one precipitating the calcites.

The Nd isotopic ratios in conjunction with the Nd and Sm contents of the celadonites, smectites, and calcites can be used to identify the source of the fluids and transport mechanisms for the REE. In general, the $^{143}Nd/^{144}Nd$ ratios for the alteration phases at 95 Ma (Fig. 8) are typical of the range for the Site 843 basalts at this time. The Sm/Nd ratios of the alteration phases (Fig. 8), especially the vein calcites, are lower than in the basalts. The lower Sm/Nd ratios cannot be explained by mixing with seawater, because they do not lie along a mixing line between the basalts and seawater (Fig. 8). The lower Sm/Nd ratios, however, can be explained by the way the REE are transported in solution.

A hydrothermal solution with seawater ionic composition and pH will transport the REE predominantly as carbonate complexes (e.g., $La(CO_3)^+$) preferentially complexing the light REE compared with the heavy REE and thus lowering the Sm/Nd ratio in the fluid compared with the source (Cantrell and Byrne, 1987). In solutions with a slightly lower pH, the metal species (e.g., La^{3+}) will predominate, but at lower concentrations than for the carbonate complexes; formation of metal species also fractionates the light REE from the heavy REE and lowers the Sm/Nd ratio, but to a lesser extent than the carbonate complexes (Cantrell and Byrne, 1987). Studies of fresh basalt glass and associated palagonite from both drill cores and dredged samples have shown that during seafloor alteration processes, Sm/Nd ratios are increased in the palagonite, and, therefore, Nd is mobilized from the glass relative to Sm (Staudigel and Hart, 1983; Bienvenu et al., 1990). As predicted by these two studies, the Sm/Nd ratios of both the vein calcites and phyllosilicates are lower than in the basalts, with the carbonates having the lowest Sm/Nd ratios (Fig. 8).

The lower Sm/Nd ratios in the phyllosilicate alteration minerals compared with the basalts suggest that the hydrothermal fluids were transporting the REE in solution. If the REE were transported as particles of palagonite that become incorporated into the celadonites and smectites, Sm/Nd would shift to values greater than those in the basalts rather than the shift to lower Sm/Nd that is observed. Taken all together, the Sr and Nd isotopes and trace elements indicate that the phyllosilicate alteration phases precipitated from hydrothermal solutions with an effective seawater/rock weight ratio of about 40, which was transporting in solution REE and other elements derived from the breakdown of basalt glass. Although the vein calcites precipitated from a more seawater-dominated hydrothermal system (water/rock ratios between 800 and 1800) and have lower Sm/Nd ratios, they do not lie on a mixing line between the basalts and seawater (Fig. 8). This result suggests that not only are the REE derived wholly from the alteration of basalt glass, but in seawater-dominated solutions the REE are transported as carbonate complexes that further fractionate the Sm/Nd ratio of the calcite compared with the phyllosilicates.

Calcites that precipitate directly from seawater should have Sr contents between 300 and 500 ppm (e.g., Staudigel et al., 1981). Site 843 vein calcites, on the other hand, have Sr contents between 46 and 121 ppm even though their $^{87}Sr/^{86}Sr$ ratios approach seawater values (Fig. 7). The low Sr abundances in vein calcites generally are attributed to a significant basalt-derived Ca component that lowers Sr/Ca in the fluids from which the calcites precipitate but without significantly affecting $^{87}Sr/^{86}Sr$ of the seawater component (e.g., Staudigel et al., 1981). The $^{143}Nd/^{144}Nd$ and Sm/Nd ratios in the vein calcite studied here do indeed require that the basalt-derived component dominate the REE in the hydrothermal fluid from which the calcite precipitated; but is this also the case for Sr/Ca?

The Sr/Ca ratios of the basalts are about 0.0015. The dark green celadonite has a basalt-like Sr/Ca ratio of 0.0015 ± 0.0001, whereas the light apple-green celadonite has a higher Sr/Ca ratio of 0.0055 ± 0.0015. On the basis of the observed changes during the initial stages of alteration of basalt glass to palagonite, Staudigel and Hart (1983) calculated fluxes of Sr and Ca from the glass with a Sr/Ca ratio of 0.002. Hart and Mottl (1983) examined fluids collected from Hole 504B basalts and extrapolated a Sr/Ca ratio of 0.0057 for the 75°C formation water end member. The Sr/Ca ratio of high-temperature (350°C) vent waters from the Galapagos Spreading Center is about 0.005 (Edmond et al., 1979). Therefore, the range of Sr/Ca ratios observed in the celadonites is comparable to those observed in the

basalts and in hydrothermal fluids and as calculated for the breakdown of basalt glass.

If the assumption is made that a vein calcite precipitates from a solution that is a mixture of seawater and the fluids from which the phyllosilicate phases precipitated, then the weight proportion of seawater in this mixture would be 11.6:1 (assuming a basalt-influenced fluid with $^{87}Sr/^{86}Sr$ of 0.7060 and 6.7-ppm Sr [Staudigel and Hart, 1983] and 95-Ma seawater with $^{87}Sr/^{86}Sr$ of 0.70734 and 8-ppm Sr). To explain both the Sr abundance and $^{87}Sr/^{86}Sr$ of the vein calcite with the lowest Sr (46 ppm), the Sr/Ca in the basalt-derived solution must be about 0.0002, based on a proportion of 11.6:1 and Sr/Ca of 0.018 for seawater. For a celadonite with Sr/Ca of 0.002 to precipitate from a solution with Sr/Ca of 0.0002, the distribution coefficient for Sr has to be an order of magnitude greater than that for Ca. Because fluids with Sr/Ca as low as 0.0002 have not been found in the basaltic crust and these fluids would have to be abundant to explain the large number of calcite veins with low Sr abundances, it seems more reasonable to assume that fluids with Sr/Ca compositions similar to those actually observed are precipitating calcites, even though this means the calcites will have an initially more basalt-like $^{87}Sr/^{86}Sr$.

Two calcites that precipitated from ~75°C ambient formation waters in Hole 504B before any drilling disturbance of the system have Sr contents of 23 and 29 ppm and $^{87}Sr/^{86}Sr$ of 0.70411 and 0.70414 (Staudigel and Hart, 1985), significantly lower than that of modern seawater ($^{87}Sr/^{86}Sr$ of 0.70907) or the extrapolated composition for the formation waters ($^{87}Sr/^{86}Sr$ of 0.70836; Hart and Mottl, 1983). These calcites from Hole 504B clearly demonstrate that precipitation occurs from fluids having a large basalt-derived component and an appropriately low Sr/Ca ratio to produce low-Sr-content calcite, but with $^{87}Sr/^{86}Sr$ ratios significantly lower than seawater values. The majority of vein calcites in older oceanic crust indicate precipitation 10–20 m.y. after the formation of the igneous crust and not precipitation ages less than 5 m.y. as do Hole 504B calcites. This suggests that these younger calcites must be redissolved at some later time. A possible explanation for the prevalence of calcite with low Sr contents and seawater $^{87}Sr/^{86}Sr$ in older crust is that early-formed calcite with 25 ppm Sr (as found in Hole 504B) later reacts with seawater by a process such as solution and redeposition to form a secondary calcite. The calcite thus can acquire the $^{87}Sr/^{86}Sr$ of the seawater with which it last equilibrated but gain little Sr. A seawater/calcite weight ratio of about 115 would explain a change in $^{87}Sr/^{86}Sr$ from 0.70450 to 0.70725 for a calcite with 30 ppm Sr; whereas the Sr content of a calcite precipitated from such a solution would increase by only 12 ppm. The Sr contents and $^{87}Sr/^{86}Sr$ ratios of the newly formed calcite vary with the relative proportions of early-formed calcite and seawater, but $^{143}Nd/^{144}Nd$ ratios will not change significantly until seawater/calcite ratios exceed values of about 7000, and by that point Sr contents are in equilibrium with the seawater Sr/Ca ratio.

The temperature range recorded by oxygen isotopes in Hole 843 vein calcites is 5°–37°C (Alt, this volume), thus indicating precipitation from low-temperature seawater-dominated fluids rather than higher-temperature 75°C fluids like those in Hole 504B. Circulation of low-temperature seawater in the oceanic crust is a late-stage event in the alteration history of the crust (e.g., Alt et al., 1986; Staudigel and Gillis, 1990; Gillis and Robinson, 1990). Because of the large volumes of seawater involved in a solution and redeposition model, the basalt-derived component in the early-formed calcite contributes only minimally to the overall oxygen isotope budget of the resulting fluid. Oxygen isotopes are therefore compatible with solution and redeposition of an early-formed calcite to form a later, low-Sr-content calcite having seawater Sr isotopes. This hypothesis is attractive because it can explain the isotopic data (O, Sr, Nd) without requiring the production of large amounts of an as yet unobserved basalt-influenced fluid with Sr/Ca less than 0.0002 and seawater Sr isotopes.

SUMMARY

An ^{40}Ar–^{39}Ar incremental heating experiment on a relatively unaltered basalt from Site 843 has yielded a crystallization age of 110 ± 2 Ma for the central Pacific Ocean igneous basement near Hawaii. Sm–Nd and Rb–Sr isotopic systematics measured on the same suite of drilled basalts are in concordance with this crystallization age. Previous estimates of the age of the basement near Hawaii inferred by indirect methods and from radiometric dates of the South Hawaiian Seamounts are too young by 20–30 m.y. Current models of past motions of the Pacific plate are probably not correct before 70 Ma, as they predict the wrong paleolatitudes for both the basement and South Hawaiian Seamounts at the times of their formation.

Phyllosilicate alteration minerals in basalts from Site 843 define an isochron with an age of 94.5 ± 0.5 Ma and an initial $^{87}Sr/^{86}Sr$ ratio of 0.70597 ± 0.00006. The isochron records the last equilibration of the phyllosilicate minerals with a hydrothermal fluid about 16 Ma after the formation of the igneous basement at 110 Ma. Calcite veins suggest that the last event recorded by the vein minerals is the sealing of the crust by a sufficient thickness of sediment to impede free circulation of seawater into the crust. The seal has been maintained for the last 95 Ma, even though recent uplift has led to new crack formation in the crust.

The $^{87}Sr/^{86}Sr$ of seawater contemporaneous with the formation of the alteration phases is established using carbonate sediments immediately above the basement. Replicate analyses give a weighted mean $^{87}Sr/^{86}Sr$ ratio of 0.70734 ± 0.00001, which agrees with previous estimates for seawater $^{87}Sr/^{86}Sr$ between 95 and 110 Ma. An average $^{143}Nd/^{144}Nd$ ratio of 0.51234, when corrected to the initial value at 95 Ma, was measured for the carbonate sediments. This $^{143}Nd/^{144}Nd$ ratio is in general agreement with previous estimates of the value in seawater and is assumed to be appropriate for this region of the Pacific Ocean from 95 to 110 Ma.

Sr and Nd isotopic ratios, in conjunction with the Sr, Nd, and Sm contents of the alteration phases, provide direct limits on the hydrothermal fluids from which they precipitate. Both the source and transportation mechanisms of the elements, and the relative proportions of seawater and basalt in the solutions can be established. Ratios such as $^{143}Nd/^{144}Nd$ and Sm/Nd in both the phyllosilicate alteration minerals and calcite veins indicate that the hydrothermal fluids transported the REE in solution as both metal species and carbonate complexes. The REE in these solutions are derived entirely from the alteration of the basalts. Sr isotopes, on the other hand, indicate variable mixtures of seawater and basalt-derived fluids during the lifetime of the hydrothermal system, with initially low water/rock ratios (~1), followed by higher water/rock ratios (~40) during the formation of the smectites and celadonites, and finally very high water/rock ratios (800–1800) during the last stage of calcite vein formation.

Calcites from veins in the oceanic crust have Sr contents too low to have precipitated directly from seawater, even though their Sr isotopes approach seawater values. In previous studies, the low Sr contents of these vein calcites have been attributed to a significant basalt-derived Ca component that lowers Sr/Ca in the fluids from which the calcites precipitate but without significantly affecting $^{87}Sr/^{86}Sr$ of the seawater component. The problem with this explanation, however, is that hydrothermal solutions with appropriately low Sr/Ca ratios and seawater Sr isotopes are not found in the basaltic crust. Moreover, although the calcite found in young oceanic crust (< 5 Ma) does have low Sr contents (20–30 ppm), its $^{87}Sr/^{86}Sr$ (~0.705) is typical of intermediate water/rock ratio (~20–40) hydrothermal systems. If such low-Sr-content calcite later reacts with seawater by a process such as solution and redeposition, the resulting calcite will have moderately low Sr contents (~40–50 ppm) as well as $^{87}Sr/^{86}Sr$ ratios approaching seawater values. If the process were to continue indefinitely, the calcite would ultimately reach equilibrium with seawater; however,

sealing of the crust by sediments usually occurs 10–20 m.y. after basement formation. The deposition and equilibration of alteration phases apparently ceases once the seal is established.

ACKNOWLEDGMENTS

I am grateful to J. Mahoney for use of the isotope laboratory at the University of Hawaii for this research. I thank K. Spencer and the other users of the isotope lab for the cooperative efforts needed to keep everything operating. I am grateful to R. Duncan at Oregon State University for providing the ^{40}Ar–^{39}Ar age dates. I want to thank A. King and M. Garcia for their collaboration in the petrochemical studies of the basalts. D. Foss helped with the reconnaissance mapping of the vein minerals using the microprobe. Discussions with J. Firth provided the paleontologic perspectives on age limits: R. Wilkens was instrumental in getting this research funded. Reviews by W. Gallahan and B. Hanan helped to improve the manuscript. This research was supported through the U.S. Science Support Program via grant TAMRF20592 for the Leg 136 post-cruise investigations. This paper is SOEST contribution number 3225.

REFERENCES*

Alt, J.C., and Honnorez, J., 1984. Alteration of the upper oceanic crust, DSDP Site 417: mineralogy and chemistry. *Contrib. Mineral. Petrol.,* 87:149–169.

Alt, J.C., Honnorez, J., Laverne, C., and Emmermann, R., 1986. Hydrothermal alteration of a 1 km section through the upper oceanic crust, Deep Sea Drilling Project Hole 504B: mineralogy, chemistry, and evolution of seawater-basalt interactions. *J. Geophys. Res.,* 91:10309–10335.

Anderson, R.N., Langseth, M.G., and Sclater, J.G., 1977. The mechanisms of heat transfer through the floor of the Indian Ocean. *J. Geophys. Res.,* 82:3391–3409.

Bass, M.N., 1976. Secondary minerals in oceanic basalt, with special reference to Leg 34, Deep Sea Drilling Project. *In* Yeats, R.S., Hart, S.R., et al., *Init. Repts. DSDP,* 34: Washington (U.S. Govt. Printing Office), 393–432.

Bienvenu, P., Bougault, H., Joron, J.L., Treuil, M., and Dmitriev, L., 1990. MORB alteration: rare-earth element/non-rare-earth hygromagmaphile element fractionation. *Chem. Geol.,* 82:1–14.

Birck, J.L., 1986. Precision K-Rb-Sr isotopic analysis: application to Rb-Sr chronology. *Chem. Geol.,* 56:73–83.

Birck, J.L., and Allègre, C.J., 1978. Chronology and chemical history of the parent body of basaltic achondrites studied by the ^{87}Rb-^{86}Sr method. *Earth Planet. Sci. Lett.,* 39:37–51.

Brocher, T.M., and ten Brink, U.S., 1987. Variations in oceanic Layer 2 elastic velocities near Hawaii and their correlation to lithospheric flexure. *J. Geophys. Res.,* 92:2647–2661.

Cantrell, K.J., and Byrne, R.H., 1987. Rare earth element complexation by carbonate and oxalate ions. *Geochim. Cosmochim. Acta,* 51:597–605.

Christensen, N.I., and Salisbury, M.H., 1972. Sea floor spreading, progressive alteration of layer 2 basalts, and associated changes in seismic velocities. *Earth Planet. Sci. Lett.,* 15:367–375.

Chyi, M.S., Crerar, D.A., Carlson, R.W., and Stallard, R.F., 1984. Hydrothermal Mn-deposit of the Franciscan Assemblages, II. Isotope and trace element geochemistry, and implications for hydrothermal convection at spreading centers. *Earth Planet. Sci. Lett.,* 71:31–45.

Clague, D.A., and Dalrymple, G.B., 1987. The Hawaiian-Emperor volcanic chain. Part I. Geologic evolution. *In* Decker, R.W., Wright, T.L., and Stauffer, P.H. (Eds.), *Volcanism in Hawaii* (Vol. 1). Geol. Surv. Prof. Pap. U.S., 1350:5–54.

Corliss, J.B., Dymond, J., Gordon, L.I., Edmond, J.M., Von Herzen, R.P., Ballard, R.D., Green, K., Williams, D., Bainbridge, A., Crane, K., and Van Andel, T.H., 1979. Submarine thermal springs on the Galapagos Rift. *Science,* 203:1073–1083.

Dalrymple, G.B., Alexander, E.C., Lanphere, M.A., and Kraker, G.P., 1981. *Irradiation of samples for ^{40}Ar–^{39}Ar dating using the Geological Survey TRIGA reactor.* Geol. Surv. Prof. Pap. U.S., 1176.

Dalrymple, G.B., Lanphere, M.A., and Clague, D.A., 1980. Conventional and $^{40}Ar/^{39}Ar$ K-Ar ages of volcanic rocks from Ojin (Site 430), Nintoku (Site 432) and Suiko (Site 433) seamounts and the chronology of volcanic propagation along the Hawaiian-Emperor Chain. *In* Jackson, E.D., Koizumi, I., et al., *Init. Repts. DSDP,* 55: Washington (U.S. Govt. Printing Office), 659–676.

Donnelly, T., Francheteau, J., Bryan, W., Robinson, P., Flower, M., Salisbury, M., et al., 1979. *Init. Repts. DSDP,* 51, 52, 53: Washington (U.S. Govt. Printing Office).

Duncan, R.A., Peterson, C., and Scheidegger, K.E., 1984. The duration of hydrothermal circulation in crust from age determinations on celadonite. *Eos,* 65:1126.

Dymond, J., and Windom, H.L., 1968. Cretaceous K/Ar ages from Pacific Ocean seamounts. *Earth Planet. Sci. Lett.,* 4:47–52.

Dziewonski, A., Wilkens, R., Firth, J., et al., 1992. *Proc. ODP, Init. Repts.,* 136: College Station, TX (Ocean Drilling Program).

Edmond, J.M., Measures, C., McDuff, R.E., Chan, L.H., Collier, R., and Grant, B., 1979. Ridge crest hydrothermal activity and the balances of the major and minor elements in the ocean. *Earth Planet. Sci. Lett.,* 46:1–18.

Elderfield, H., 1976. Hydrogenous material in marine sediments; excluding manganese nodules. *In* Riley, J.P., and Chester, R. (Eds.), *Chemical Oceanography* (Vol. 5): New York (Academic Press), 137–208.

Engebretson, D.C., Cox, A., and Gordon, R.G., 1985. *Relative Motions Between Oceanic and Continental Plates in the Pacific Basin.* Spec. Pap.—Geol. Soc. Am., 206.

Epp, D., 1978. Age and tectonic relationships among volcanic chains on the Pacific plate [Ph.D. dissert.]. Univ. of Hawaii, Honolulu.

————, 1984. Implications of volcano and swell heights for thinning of the lithosphere by hotspots. *J. Geophys. Res.,* 89:9991–9996.

Ewing, J., and Houtz, R., 1979. Acoustic stratigraphy and structure of the oceanic crust. *In* Talwani, M., Harrison, C.G., and Hayes, D.E. (Eds.), *Deep Drilling Results in the Atlantic Ocean: Ocean Crust.* Am. Geophys. Union, Maurice Ewing Ser., 1:1–14.

Faure, G., 1986. *Principles of Isotope Geology:* New York (Wiley).

Freedman, A.P., and Parson, B., 1986. Seasat-derived gravity over the Musician Seamounts. *J. Geophys. Res.,* 91:8325–8340.

Gallahan, W.E., and Duncan, R.A., 1991. K-Ar ages of celadonites from the Troodos Ophiolite, Cyprus: a new estimate for the duration of hydrothermal alteration in oceanic crust. *Eos,* 72:453.

Gillis, K.M., and Robinson, P.T., 1990. Patterns and processes of alteration in the lavas and dykes of the Troodos Ophiolite, Cyprus. *J. Geophys. Res.,* 95:21523–21548.

Goldberg, D., and Moos, D., 1992. Physical properties of 110 Ma oceanic crust at Site OSN-1: implications for emplacement of a borehole seismometer. *Geophys. Res. Lett.,* 19:757–760.

Harland, W.B., Armstrong, R.L., Cox, A.V., Craig, L.E., Smith, A.G., and Smith, D.G., 1990. *A Geologic Timescale, 1989:* Cambridge (Cambridge Univ. Press).

Hart, S.R., and Mottl, M.J., 1983. Alkali and Sr isotope geochemistry of waters collected from basaltic basement, Deep Sea Drilling Project Site 504B, Costa Rica Rift. *In* Cann, J.R., Langseth, M.G., Honnorez, J., Von Herzen, R.P., White, S.M., et al., *Init. Repts. DSDP,* 69: Washington (U.S. Govt. Printing Office), 487–494.

Hart, S.R., and Staudigel, H., 1978. Oceanic crust: age of hydrothermal alteration. *Geophys. Res. Lett.,* 5:1009–1012.

————, 1979. Ocean crust-seawater interaction: Sites 417 and 418. *In* Donnelly, T., Francheteau, J., Bryan, W., Robinson, P., Flower, M., Salisbury, M., et al., *Init. Repts. DSDP,* 51, 52, 53 (Pt. 2): Washington (U.S. Govt. Printing Office), 1169–1176.

————, 1986. Ocean crust vein mineral deposition: Rb/Sr ages, U-Th-Pb geochemistry, and duration of circulation at DSDP Sites 261, 462 and 516. *Geochim. Cosmochim. Acta,* 50:2751–2761.

Hess, J., Bender, M.L., and Schilling, J.G., 1986. Evolution of the ratio of strontium-87 to strontium-86 in seawater from Cretaceous to Present. *Science,* 231:979–984.

Houtz, R., and Ewing, J., 1976. Upper crustal structure as a function of plate age. *J. Geophys. Res.,* 81:2490–2498.

Jacobson, R.S., 1992. Impact of crustal evolution on changes of the seismic properties of the uppermost ocean crust. *Rev. Geophys.,* 30:23–42.

Johnson, D.A., 1972. Ocean-floor erosion in the equatorial Pacific. *Geol. Soc. Am. Bull.,* 83:3121–3144.

Karato, S., and Becker, K., 1983. Porosity and hydraulic properties of sediments from the Galapagos Spreading Center and their relation to hydrothermal circulation in the oceanic crust. *J. Geophys. Res.,* 88:1009–1017.

* Abbreviations for names of organizations and publications in ODP reference lists follow the style given in *Chemical Abstracts Service Source Index* (published by American Chemical Society).

Koepnick, R.B., Burke, W.H., Denison, R.E., Hetherington, E.A., Nelson, H.F., Otto, J.B., and Waite, L.E., 1985. Construction of the seawater $^{87}Sr/^{86}Sr$ curve for the Cenozoic and Cretaceous: supporting data. *Chem. Geol. (Isotope Geosci. Sect.),* 58:55–81.

Lancelot, Y., and Larson, R.L., 1975. Sedimentary and tectonic evolution of the northwestern Pacific. *In* Larson, R.L., Moberly, R., et al., *Init. Repts. DSDP,* 32: Washington (U.S. Govt. Printing Office), 925–939.

Lanphere, M.A., and Dalrymple, G.B., 1978. The use of $^{40}Ar/^{39}Ar$ data in evaluation of disturbed K-Ar systems. *In* Zartman, R.E. (Ed.), *Short Papers of the Fourth International Conference, Geochronology, Isotope Geology.* Open-File Rep.— U.S. Geol. Surv., 78-701:241–243.

Lawrence, J.R., and Gieskes, J.M., 1981. Constraints on water transport and alteration in the oceanic crust from the isotopic composition of pore water. *J. Geophys. Res.,* 86:7924–7934.

Lawrence, J.R., Gieskes, J.M., and Broecker, W.S., 1975. Oxygen isotope and cation composition of DSDP pore water and the alteration of layer II basalts. *Earth Planet. Sci. Lett.,* 27:1–10.

LeHuray, A.P., and Johnson, E.S., 1989. Rb-Sr systematics of Site 642 volcanic rocks and alteration minerals. *In* Eldholm, O., Thiede, J., Taylor, E., et al., *Proc. ODP, Sci. Results,* 104: College Station, TX (Ocean Drilling Program), 437–448.

Lindwall, D., 1991. Old Pacific crust near Hawaii: a seismic view. *J. Geophys. Res.,* 96:8191–8203.

Lister, C.R.B., 1977. Qualitative models of spreading-center processes including hydrothermal penetration. *Tectonophysics,* 37:203–218.

Lugmair, G.W., Scheinen, N.B., and Marti, K., 1975. Sm-Nd age and history of Apollo 17 basalt 75075: evidence for early differentiation of the lunar exterior. *Proc. 6th Lunar Sci. Conf., Geochim. Cosmochim. Acta,* 6:1419–1429.

Mahoney, J., Nicollet, C., and Dupuy, C., 1991. Madagascar basalts: tracking oceanic and continental sources. *Earth Planet. Sci. Lett.,* 104:350–363.

Mahoney, J.J., 1987. An isotopic survey of Pacific oceanic plateaus: implications for their nature and origin. *In* Keating, B.H., Fryer, P., Batiza, R., and Boehlert, G.W. (Eds.), *Seamounts, Islands, and Atolls.* Am. Geophys. Union Monogr., 43:207–220.

McDougall, I., and Harrison, T.M., 1988. *Geochronology and Thermochronology by the $^{40}Ar/^{39}Ar$ Method:* New York (Oxford Univ. Press).

McIntyre, G.A., Brooks, C., Compston, W., and Turek, A., 1966. The statistical assessment of Rb-Sr isochrons. *J. Geophys. Res.,* 71:5459–5468.

Michard, A., Albarède, F., Michard, G., Minster, J.F., and Charlou, J.L., 1983. Rare-earth and uranium in high-temperature solutions from East Pacific Rise hydrothermal vent field (13°N). *Nature,* 303:795–797.

Mottl, M.J., Anderson, R.N., Jenkins, W.J., and Lawrence, J.R., 1983. Chemistry of waters sampled from basaltic basement in Deep Sea Drilling Project Holes 501, 504B, and 505B. *In* Cann, J.R., Langseth, M.G., Honnorez, J., Von Herzen, R.P., White, S.M., et al., *Init. Repts. DSDP,* 69: Washington (U.S. Govt. Printing Office), 475–483.

Mottl, M.J., Lawrence, J.R., and Keigwin, L.D., 1983. Elemental and stable-isotope composition of pore waters and carbonate sediments from Deep Sea Drilling Project Sites 501/504 and 505. *In* Cann, J.R., Langseth, M.G., Honnorez, J., Von Herzen, R.P., White, S.M., et al., *Init. Repts. DSDP,* 69: Washington (U.S. Govt. Printing Office), 461–473.

Peterson, C., Duncan, R., and Scheidegger, K.F., 1986. Sequence and longevity of basalt alteration at Deep Sea Drilling Project Site 597. *In* Leinen, M., Rea, D.K., et al., *Init. Repts. DSDP,* 92: Washington (U.S. Govt. Printing Office), 505–515.

Piepgras, D.J., and Jacobsen, S.B., 1988. The isotopic composition of neodymium in the North Pacific. *Geochim. Cosmochim. Acta,* 52:1373–1381.

Piepgras, D.J., and Wasserburg, G.J., 1980. Neodymium isotopic variations in seawater. *Earth Planet. Sci. Lett.,* 50:128–138.

————, 1982. The isotopic composition of neodymium in waters from the Drake Passage. *Science,* 217:207–214.

Pringle, M.S., Jr., 1992. Geochronology and petrology of the Musicians Seamounts, and the search for hot spot volcanism in the Cretaceous Pacific [Ph.D. dissert.]. University of Hawaii, Manoa.

Pringle, M.S., Staudigel, H., and Gee, J., 1991. Jasper Seamount: seven million years of volcanism. *Geology,* 19:364–368.

Richardson, S.H., Hart, S.R., and Staudigel, H., 1980. Vein mineral ages of old oceanic crust. *J. Geophys. Res.,* 85:7195–7200.

Richter, F.M., and DePaolo, D.J., 1987. Numerical models for diagenesis and the Neogene Sr isotopic evolution of seawater from DSDP Site 590B. *Earth Planet. Sci. Lett.,* 83:27–38.

————, 1988. Diagenesis and Sr isotopic evolution of seawater using data from DSDP 590B and 575. *Earth Planet. Sci. Lett.,* 90:382–394.

Sager, W.W., and Pringle, M.S., 1987. Paleomagnetic constraints on the origin and evolution of the Musicians and South Hawaiian seamounts, central Pacific Ocean. *In* Keating, B.H., Fryer, P., Batiza, R., and Boehlert, G.W. (Eds.), *Seamounts, Islands and Atolls.* Am. Geophys. Union, Geophys. Monogr. Ser., 43:133–162.

Samson, S.D., and Alexander, E.C., Jr., 1987. Calibration of the interlaboratory $^{40}Ar/^{39}Ar$ dating standard, MMhb-1. *Chem. Geol.,* 66:27–34.

Scheidegger, K.F., and Stakes, D.S., 1980. X-ray diffraction and chemical study of secondary minerals from Deep Sea Drilling Project Leg 51 Holes 417A and 417D. *In* Donnelly, T., Francheteau, J., Bryan, W., Robinson, P., Flower, M., Salisbury, M., et al., *Init. Repts. DSDP,* 51, 52, 53 (Pt. 2): Washington (U.S. Govt. Printing Office), 1253–1263.

Schwank, D.C., and Lazarewicz, A.R., 1982. Estimation of seamount compensation using satellite altimetry. *Geophys. Res. Lett.,* 9:907–910.

Sclater, J.G., Anderson, R.N., and Bell, M.L., 1971. Elevation of ridges and evolution of the central Eastern Pacific. *J. Geophys. Res.,* 76:7888–7915.

Stakes, D.S., and Scheidegger, K.F., 1981. Temporal variations in secondary minerals from Nazca Plate basalts. *In* Kulm, L.D., Dymond, J., Dasch, E.J., Hussong, D.M., and Roderick, R. (Eds.), *Nazca Plate: Crustal Formation and Andean Convergence.* Mem.—Geol. Soc. Am., 154:109–130.

Staudigel, H., Doyle, P., and Zindler, A., 1985. Sr and Nd isotopic systematics in fish teeth. *Earth Planet. Sci. Lett.,* 76:45–46.

Staudigel, H., and Gillis, K., 1990. The timing of hydrothermal alteration in the Troodos ophiolite. *In* Malpas, J., Moores, E.M., Panayiotou, A., and Xenophontos, C. (Eds.), *Ophiolites: Oceanic Crustal Analogues.* Nicosia, Cyprus, Geol. Surv., 665–672.

Staudigel, H., Gillis, K., and Duncan, R., 1986. K/Ar and Rb/Sr ages of celadonites from the Troodos ophiolite, Cyprus. *Geology,* 14:72–75.

Staudigel, H., and Hart, S.R., 1983. Alteration of basaltic glass: mechanisms and significance for the oceanic crust-seawater budget. *Geochim. Cosmochim. Acta,* 47:337–350.

————, 1985. Dating of ocean crust hydrothermal alteration: strontium isotope ratios from Hole 504B carbonates and a reinterpretation of Sr isotope data from Deep Sea Drilling Project Sites 105, 332, 417, and 418. *In* Anderson, R.N., Honnorez, J., Becker, K., et al., *Init. Repts. DSDP,* 83: Washington (U.S. Govt. Printing Office), 297–303.

Staudigel, H., Hart, S.R., and Richardson, S.H., 1981. Alteration of the oceanic crust: processes and timing. *Earth Planet. Sci. Lett.,* 52:311–327.

Steiger, R.H., and Jäger, E., 1977. Subcommission on geochronology: convention on the use of decay constants in geo- and cosmochronology. *Earth Planet. Sci. Lett.,* 36:359–362.

Tlig, S., 1982. Géochemie comparée de sédiments de l'océan Indien et de l'océan Pacifique—intérêt du fractionnement minérologique et de l'étude de plusieurs groupes d'éléments dosés par activation neutronique. [Ph.D. dissert.]. Univ. of South Paris, Orsay.

Von Damm, K.L., Edmond, J.M., Grant, B., Measures, C.I., Walden, B., and Weiss, R.F., 1985. Chemistry of submarine hydrothermal solution at 21°N. East Pacific Rise. *Geochim. Cosmochim. Acta,* 49:2197–2220.

Watts, A.B., Bodine, J.H., and Ribe, N.M., 1980. Observations of flexure and the geological evolution of the Pacific Ocean Basin. *Nature,* 283:532–537.

Wilkens, R.H., Fryer, G.J., and Karsten, J., 1991. Evolution of porosity and seismic structure of upper oceanic crust: importance of aspect ratios. *J. Geophys. Res.,* 96:17891–17995.

Wolery, T.J., and Sleep, N.H., 1976. Hydrothermal circulation and geochemical flux at mid-ocean ridges. *J. Geol.,* 84:249–275.

York, D., 1969. Least squares fitting of a straight line with correlated errors. *Earth Planet. Sci. Lett.,* 5:320–324.

Date of initial receipt: 4 December 1992
Date of acceptance: 28 June 1993
Ms 136SR-212